博士論文

Elucidation of the Role of T-bet Overexpression in T cells in the Development of Acquired Pulmonary Alveolar Proteinosis

（後天性肺胞蛋白症発症における T 細胞内 T-bet 過剰発現の役割解明）

入口　翔一

Table of Contents

Abbreviations (Listed in an alphabetical order)

Abca1	ATP-Binding Cassette Sub-family A member 1
Abcg1	ATP-Binding Cassette Sub-family G member 1
AF	Autofluorescence
ANOVA	Analysis of variance
APC	allophycocyanin
Bach2	BTB and CNC homology 1, basic leucine zipper transcription factor 2
BAL	Bronchoalveolar lavege
BM	Bone marrow
CBA	Cytometric beads array
CBC	Complete blood count
CCR2	C-C chemokine receptor type 2
CD	Cluster of differentiation
CFC	Colony-forming cell
CFU	Colony-forming unit
CMP	Common myeloid progenitor
CSF	Colony-stimulating factor
Cy	Cyan
DAB	3,3'-diaminobenzidine
DNA	Deoxyribonucleic acid
EDTA	Ethylenediaminetetraacetic acid
FACS	Fluorescence activated cell sorting
FBS	Fetal bovine serum
FCM	Flowcytometer
FITC	Fluorescein isothiocynate
GM-CSF	granulocyte-macrophage colony-stimulating factor
GM-CSFRα	GM-CSF receptor alpha chain
GM-CSFRβc	GM-CSF recepor beta chain (a.k.a. common beta chain)
GMP	Granulocyte/macropahge progenitor
H&E	Hematoxylin and eosin
HPC	Hematopoietic progenitor cell
HSC	Hematopoietic stem cell
HSPC	Hematopoietic stem/progenitor cell
IFN-γ	Interferon-gamma
IL	Interleukin
Lin	Lineage markers
M-CSF	Macrophage-CSF
MCP-1	Monocyte chemoattractant protein-1
MDP	Monocyte/dendritic cell progenitor
MDS	Myelodysplastic syndrome
MEP	Megakaryocyte/erythroid progenitor
MHC	Major histocompatibility complex
NOS	Nitric oxide synthase
PAP	Pulmonary Alveolar Proteinosis
PAS	Periodic acid staining

PB	Peripheral Blood
PBS	Phosphate-buffered saline
PCR	Polymerase chain reaction
PE	Phycoerythrin
PerCP	Peridinin chlorophyll
Rag	Recombination-activating gene
Pparγ	Peroxisome Proliferator-Activated Receptor gamma
RNA	Ribonucleic acid
SNK	Student-Newman-Keuls
SP	Surfactant protein
T-bet	T-box transcription factor (a.k.a. Tbx21)
tg	Transgenic
Th	Helper T
Th1	Type 1 helper T
Th17	IL-17-producing T
Th2	Type 2 helper T
TNF	Tumor necrosis factor
Treg	Regulatory T
WBC	White blood cell
WBMC	Whole bone marrow cell
WT	Wild-type

Chapter 1: Introduction

1.1 Pulmonary Alveolar Proteinosis

Pulmonary alveolar proteinosis (PAP) is a rare lung disorder characterized by the accumulation of surfactant in the alveolar spaces due to functional defects in alveolar macrophages, a tissue-resident macrophages in the lung (1, 2). The disease results in varying degree of respiratory insufficiency and an increased susceptibility to infection due to defects in alveolar macrophage- and neutrophil-mediated host defense. Although open-lung biopsy remains the "gold standard" for diagnosis, the procedure has become less common because a diagnosis of PAP can be established in about 75% of suspected cases by the characteristic finding of milky appearance from bronchoalveolar lavege (BAL)(3). The milky effluent comprises acellular eosinophilic material with morphologically abnormal "foamy" macrophages(4). The characteristic features of lung biopsy specimen from PAP patients include the filling of the alveolar spaces with Periodic acid staining (PAS)-positive surfactant. A mild lymphocyte infiltration into the interstitial spaces was also reported, but its association with the disease is unknown (5).

1.2 Epidemiology

According to a study conduced by Ben-Dov *et al*., the estimated prevalence of acquired PAP was reported to be 0.37 per 100,000 persons (1, 2, 6). The acquired form comprises more than 90 percent of the reported cases (see **1.4 Pathogenesis** for more details) (3, 5, 7-9). With such a low annual incidence, it is extremely difficult to accumulate significant cases for comprehensive experience. In fact, more than 75 percent of reported cases comprise single case or small case series and there are only five publications reporting case series of ten or more. Male shows higher prevalence than female, possibly due to more frequent smoking habits (1, 2, 4, 5).

1.3 Pulmonary surfactant

Pulmonary surfactant is comprised of ~90% of phospholipids and ~10% of surfactant proteins (SP-A, -B, -C, and –D). Pulmonary surfactant is vital to lung structure and functions in such ways that it prevents alveolar collapse and contributes to host defense (3, 5, 10). Maintaining the balance between the productions by alveolar type II epithelial cells and clearance by both alveolar macrophages and, to a lesser extent, alveolar type II epithelial cells are the prerequisite for proper lung functions. Indeed, disruption of surfactant homeostasis causes PAP and disorders of surfactant production (DSP). DSP is caused by genetic mutations in the genes encoding SP-B, SP-C, or ABCA3, and often exhibit more severe and fetal clinical course compared to PAP (4, 11, 12).

1.4 Pathogenesis

The pathogenesis of PAP has remained enigmatic since its initial description in 1958 (1). An important step forward in better understanding of the pathogenesis of PAP was the observations that the clinical disease states are comprised of three distinct subgroups: hereditary, secondary, and autoimmune forms. Over 90% of all cases of PAP occur as an acquired disorder, which includes secondary and autoimmune forms. However, molecular pathogenesis of PAP remained unknown until mice deficient in the genes encoding granulocyte-macrophage colony-stimulating factor (GM-CSF) or the beta chain of its receptor have shown to develop a disease identical to human PAP (2, 5, 13, 14). Followed by the seminal findings, subsequent studies have revealed that the molecular pathogenesis in most of the cases of PAP is due to the disruption of granulocyte-macrophage colony-stimulating factor (GM-CSF) signaling (1, 2, 6, 15-17). Likewise, hereditary PAP has been attributed to abnormalities or loss of GM-CSF receptor alpha chain (3, 5, 7-9, 16, 18). It has also been demonstrated that the pathogenesis of autoimmune PAP, the most common cause of

disease, is recognized by the presence of high levels of neutralizing GM-CSF autoantibodies (19).

1.5 GM-CSF signaling

GM-CSF is a hematopoietic cytokine known to stimulate various functions in immature and mature hematopoietic cells. In the lung, alveolar type II epithelial cells also produce GM-CSF (20). GM-CSF is present in other tissues and serum, although the amount is maintained at a low concentration. It binds to its heteromeric receptor comprised of a low-affinity α chain and an affinity-converting β chain. Ligand binding initiates signal transduction including Janus kinase 2 (JAK2)-the signal activator of transcription-5 (STAT5) (21, 22). In addition, ligand-mediated JAK2 autophosphorylation also induces mitogen-activated protein kinase, phosphatidylinositol 3-kinase, and other unknown pathways (23-26). Further investigations with GM-CSF deficient mice have demonstrated its roles in surfactant catabolism, immune functions, and terminal differentiation of alveolar macrophages particularly through PU.1, although the upstream signal has not been identified (27, 28).

1.6 Secondary PAP

In comparison to the hereditary and autoimmune forms, little is known about the pathogenesis of secondary PAP. The underlying diseases include hematological disorders, immunological diseases, infections, and various toxic inhalation syndromes. For example, its association with myelodysplastic syndrome (MDS) has been well documented (2, 13, 14, 29). In 2008, a national cross-sectional study in Japan has shown that the incidence of secondary PAP comprises 9.7% of the PAP syndrome (15-17, 30). An important indication has been reported by Ishii *et al.* that the prognosis of secondary PAP is worse than that of autoimmune PAP (16, 18, 31). The pathogenesis of secondary PAP is poorly understood. A previous study

has shown a development of PAP in patients with myelodysplasia together with defects in GM-CSF signaling, suggesting that GM-CSF signaling disruption involves in the pathogenesis of some secondary PAP cases (19, 32). Nonetheless, development of secondary PAP without GM-CSF signaling has been reported (33). Taken together, these findings indicate PAP occurs independently of GM-CSF signaling defects, but its pathogenesis remains unknown.

1.7 PAP development and T cell overactivation

The observations that secondary PAP is known to develop in a fraction of the patients with hematological disorders, immunological diseases, and infections suggest a link between dysregulation of the immune-hematopoietic systems and the development of PAP. Consistent with these observations, an increase in the number of both CD4 and CD8 T cells has been observed in brochoalveolar lavage (BAL) fluids of the PAP patients studied compared to healthy individuals (34). Furthermore, an abnormal activation of T cells, characterized by expressions of HLA-DR and IL-2R, has been reported in PAP patients (35). These findings indicate that aberrant T cell activation plays significant roles in the pathogenesis of PAP.

1.8 T-bet

T cell activation is modulated by distinct transcription factors. Among them, T-bet is known as a T cell transcription factor regulating Th1 cell differentiation/activation program (36). Naïve $CD4^+$ T cells differentiate into different subsets, such as Th1, Th2, Th17, follicular helper T and Treg cells in response to distinct stimuli provided from cells of innate immunity as well as the signals driven by a MHC:peptide complex. T-bet not only promotes the expression of the Th1 cytokine, IFN-γ, in activated $CD4^+$ T cells, but also is a critical regulator for controlling type1 immune and inflammatory responses by coordinating the gene

expressions in other immune cells (37). Besides its role in Th1 differentiation, it has been shown that T-bet is expressed in other cells of the innate and adaptive immune system and its expression is required for the survival, development, and effector functions of those cells. For example, T-bet regulates effector functions and the development of $CD8^+$ T cell memory (38-40).

1.9 T-bet and diseases

Dysregulation of T-bet expression has been implicated in immunopathology and the development of autoimmunity. For example, aberrant T-bet expressions can be a driving force in inflammatory diseases, including inflammatory bowel disease, experimental autoimmune encephalomyelitis, arthritis, systemic lupus erythematosus and type 1 diabetes (41). Several studies have reported augmented IFN-γ production and T-bet expression in $CD4^+$ T cells infiltrating affected lesions in patients with Crohn's disease (42, 43). T-bet-mediated expression of IFN-γ also appears to play a key role in the pathogenesis of type 1 diabetes, an organ-specific autoimmune disease (44). Notably, a considerable number of aplastic anemia patients show constitutive expression of T-bet, though the mechanism by which this occurs remains unclear (45-47). By contrast, T-bet deficient mice have increased susceptibility to many intracellular microorganisms and to asthma and allergies (48). Therefore, understanding the roles of T-bet expression in such diseases will be beneficial in developing the new therapeutics.

1.10 Aim of the study

Despite the effects of T-bet deficiency on the immune system have been extensively studied, the roles of its overexpression remain to be explored. In addition, it is possible that aberrant T cell activation by dysregulated T-bet expression involves other immune and hematological

disorders. Those previous studies prompter us to consider the possibility that overactivation of T cells by T-bet overexpression could involve in the disease progression or initiation of PAP. To this end, the human CD2 (hCD2)-T-bet-transgenic (CD2-T-bet tg) mice have been generated and used to study the roles of T-bet in the pathogenesis of inflammatory diseases. The expression of T-bet in the mice is regulated under the control of human CD2 promoter, thereby allowing its expression only in T cells (49). A recent study utilizing this transgenic mouse line has shown a suppressive role of T-bet in the development of arthritis (50). Other study has demonstrated that both $CD4^+$ and $CD8^+$ T cells from the CD2-T-bet tg mice indeed produce aberrant amounts of IFN-γ and contribute to spontaneous skin inflammation that leads to contact dermatitis development (51). However, other organs of the mice have not been fully investigated. In the current study, we further explored the CD2-T-bet tg mouse with a particular focus on the hematopoietic and the respiratory systems and found that only the aged transgenic mice homozygous for the human CD2-T-bet transgene allele spontaneously developed PAP-like disease accompanied by functional conversion of macrophages in the lung.

Chapter 2: Materials and Methods

2.1 Animals and samples

Generation of the CD2-T-bet transgenic lines has been described previously (51). T-bet transgenic mice were inbred with C57BL/6 mice for at least eight generations before use in experiments. DNA was extracted from the tail of each mouse by NaOH extraction and each genotype was subsequently determined by polymerase chain reaction (PCR) using specific primers (Table 1). Mice were maintained in specific pathogen-free conditions in the laboratory animal center. All experiments were performed according to the Guide for the Care and Use of Laboratory Animals at the University of Tokyo. All animal experiments were approved by Institutional Animal Care and Use Committee.

2.2 Histopathological analysis

Murine tissues were fixed in 4% paraformaldehyde for 72 hours at 4°C, dehydrated in alcohol, cleared in xylene, and paraffinized by an automated processor. The tissue sections (4 μm) from paraffin-embedded tissue blocks were placed on slides, deparaffinized in xylene, redehydrated through graded alcohol solutions (100%, 90%, 80%, 70%, and 50%), and then stained with PAS or hematoxylin and eosin.

2.3 Bronchoalveolar lavage (BAL)

The lungs were lavaged with six sequential aliquots of 1 ml PBS. The first lavage was used for cytokine assays. Total cells were counted with a hemocytometer and differential cell counts were obtained after staining with Hemacolor (Merck).

2.4 Immunohistochemistry

After incubation with 3% hydrogen peroxide to inhibit endogenous peroxidase activity, lung

sections were immunostained with anti-surfactant protein (SP)-A (1:200, ab115791, Abcam, Cambridge, MA), and polyclonal antibodies. The sections were developed using Histofine MAX PO(R) (Nichirei Biosciences, Tokyo, Japan) and a DAB solution according to the manufacturer's instruction. Finally, the sections were counterstained with hematoxylin.

2.5 PCR

To analyze gene expressions, total RNA was extracted from macrophages or whole lung tissues using RNeasy Mini Kit (Qiagen). The RNA was reverse transcribed using PrimeScript II 1sr strand cDNA Synthesis Kit (TAKARA) using random hexamers. Quantitative real-time PCR was performed in a sequence detector ABI7500 Fast or StepOne Plus realtime PCR Systems (Applied Biosystems) using following primers: GM-CSFRa forward 5'-cctgctcttctccacgctac-3', and reverse 5'-ggtcgaaggtcaggttgagg-3'; GM-CSFRbc forward 5'-aggaagagcctgcaactcac-3', and reverse, 5'-ttccctcctagactgcatcc-3'; GM-CSF, forward 5'-atgcctgtcacgttgaatga-3', and reverse, 5'-ccgtagaccctgctcgaata-3'; PU.1, forward 5'-tgcaaaatggaagggttttc-3', and reverse 5'-aaccaagtcatccgatggag-3'; Actb, forward 5'-ctaaggccaaccgtgaaaag-3', and reverse 5'-accagaggcatacagggaca-3'; Pparg, forward 5'-gaaagacaacggacaaatcacc-3', and reverse 5'-gggggtgatatgtttgaacttg-3'; Abca1, forward 5'-atcgaagccgtctttccag-3', and reverse 5'-ccagtatgacttggtacaaggaaa-3'; Abcg1, forward 5'-gggtctgaactgccctacct-3' and reverse 5'-tactcccctgatgccacttc-3'; and Bach2, forward 5'-ggattgctgtagccttctcatc-3', and reverse 5'-agacatgccgttcaaaccat-3'.

2.6 Microarray analysis

The RNAs from the lungs were extracted using RNeasy Mini Kit (Qiagen, Venlo, the Netherland). The RNA was reverse transcribed using ReverTra Ace qPCR RT Master Mix (TOYOBO, Osaka, Japan). The prepared cRNAs were hybridized with an Agilent microarray

slide (Whole Mouse Genome) according to the manufacturer's instruction (Agilent technologies, Santa Clara, CA, U.S.A.), after which it was scanned with scanner. The obtained data were analyzed using GeneSpring software (Agilent technologies).

2.7 Transplantation of splenocytes

For adoptive transfer experiments, splenocytes were harvested from the spleens of *T-bet*$^{tg/tg}$, *T-bet*$^{tg/wt}$, and WT mice, crushed with syringe, and then passed through nylon mesh to obtain single-cell suspensions. The mononuclear cells among the splenocytes were obtained via gravity centrifugation with Ficol-Paque PLUS (GE Healthcare) at 1:1 (vol/vol) ratio. A total of 1 x 10^6 purified mononuclear cells was then intravenously injected into CD45.1-*Rag2*$^{-/-}$ mice (Sankyo Laboratories, Ibaraki, Japan). From the 5th week after transplantation, the mice were subjected to weekly monitoring of their peripheral blood total complete blood count (CBC), and flow cytometric analyses to detect T-cell engraftment and subpopulations of myeloid cells. The mice were analyzed at the 40th week after transplantation as described in donor mice analyses.

2.8 Adoptive Transfer of T cells

To adoptively transfer T cells from T-bet tg mice, splenocytes were harvested from the spleen and were positively selected against CD3ε (clone: 145-2C11) using MACS LS columns and MicroBeads according to the manufacturer's instructions (Miltenyi Biotec, Auburn, CA). Briefly, the harvested cells were stained with PE conjugated-anti-mouse CD3ε antibody for 15 min. at room temperature and subsequently stained with anti-PE MicroBeads antibody (Mat. no.: 120-000-294, Miltenyi Biotec) for 15 min. at 4°C. The stained cells were then selected against the CD3ε expression through LS column and the positive fraction in the column was collected with the plunger. A total of 5 x 10^5 cells/200 μl of PBS was

intravenously injected into each CD45.1-*Rag2*$^{-/-}$ mouse. The periodical peripheral blood examinations were performed as described in 2.10.

2.9 Cytometric Beads Array (CBA)

Some samples were applied to a Mouse Inflammation and a Mouse Th1/Th2/Th17 Cytokine kits (BD Biosciences) using FACS Canto II (BD Biosciences) and BD CBA software according to the manufacturer's instructions. Data were analyzed using BD FCAP Array software. Standard curves were constructed using four-parameter logistic curve fitting to calculate cytokine concentrations.

2.10 Flow Cytometry

BAL-recovered cells were collected as described in 2.3. The spleen was crushed and passed through nylon mesh to obtain single-cell suspensions. A femur was harvested and the marrow was flushed out by 2ml of PBS. The BAL cells were diluted to $2x10^6$/100 μl and incubated with a non-specific-binding blocking reagent containing mouse CD16/CD32 (2.4G2) for 15 min at 4°C. The collected cells were stained with antibodies indicated below for 30 min at 4°C and subsequently analyzed on either a FACSAria II or FACSAria (BD Bioscience, San Jose, CA). Data were analyzed by FlowJo software (TreeStar).

Cells were stained with the following directly conjugated antibodies for flow cytometric analysis: fluorescein isothiocynate (FITC)-anti-Ly6C (AL-21, BD Pharmingen, San Deigo, CA), phycoerythrin (PE)-anti-Siglec-F (E50-2440, BD Pharmingen), PE/Cy7- and APC/Cy7-anti-Gr-1 (RB6-8C5, eBiosciecne), allophycocyanin (APC)-anti-CD11c (N418, BioLegend, San Diego, CA), PE/Cy7- and APC/Alexa e-fluor 750-anti-CD11b (M1/70, eBioScience), PE-anti-F4/80 (CI:A3-1, BioLegend), PerCP/Cy5.5- and PE/Cy7-anti-B220 (RA3-6B2, eBioscience), Pacific Orange-anti-CD8α (53-6.7, eBioscience), APC-anti-CD3ε (145-2C11,

eBioscience), and Alexa Fluor 405-anti-CD4 (RM4-5, CALTAG Laboratories). For weekly monitoring of splenocyte-transplanted mice, we used FITC or Pacific Blue-anti-CD45.2 (104, BioLegend), biothylated-anti-CD45.1 (A20, BioLegend), APC/Cy7 or PerCP/Cy5.5-anti-StreptAvidin (Streptavidin, both from BioLegend). For hematopoietic stem/progenitor cell population analysis, FITC-anti-CD115 (AFS98, eBioscience), PE-anti-CD150 (TC15-12F2.2, Biolegend), PE/Cy7-anti-Sca-1 (D7, eBioscience), APC-anti-c-kit (2B8, eBioscience), and Alexa 700-anti-CD34 (RAM34, eBioscience). The lineage marker cocktail contained the following biothylated antibodies: anti-mouse Gr-1, Ter119 (TER-119, eBioscience), CD4, CD8, B220, IL-7Rα (A7R34, Biolegend).

2.11 Phagocytosis assays

BAL-recovered cells were plated in a 24-well plastic plate. After 1 h of incubation at 37°C, the cells were washed three times with warm PBS to remove non-adherent cells. The adherent cells (5 x 10^5/well) were incubated with latex microbeads labeled with FITC at 5 x 10^7/well (0.75 μm diameter; Polysciences, Inc. Warrington, PA). After 2 h incubation at 37 °C, the cells were washed, fixed with 2.5% paraformaldehyde for 20 min, and the percentage of macrophages that bound/engulfed beads was determined by flow cytometry.

2.12 Peripheral blood examinations

Peripheral blood (PB) was collected from the retro-orbital cavity using a non-heparinized glass capillary and then transferred into a 1.5mL tube containing 1μl of 0.5 M EDTA (pH 8.0). The total CBC was obtained by an automated counter (CelltacαEK-6358; Nihon Kohden, Tokyo, Japan). For flowcytometric analysis of PB, red blood cells were lysed with ammonium chloride solution at room temperature for 15 min, followed by a centrifugation at 400 x g for 5min. The pellets were stained with a cocktail of diluted directly conjugated

fluorescent antibodies described above at room temperature for 15 min. The cells were washed with PBS containing 3% (vol/vol) FBS, centrifuged, and resuspended in the same buffer with 1 μg/ml of propidium iodide.

2.13 CFC assays

Bone marrow cells isolated from the femur and tibia were seeded at a density of 5 x 10^4 cells/35-mm dish in methylcellulose medium (Methocult M3234; Stem Cell Technologies, Vancouver, Canada) supplemented with 50 ng/ml murine stem cell factor (Peprotech, Rocky Hill, NJ, U.S.A.), 10 ng/ml IL-3 (Peprotech), 10 ng/ml IL-6 (R&D Systems, Minneapolis, MN), 3 U/ml erythropoietin (Peprotech), and 30 U/ml thrombopoietin (Peprotech). Then, the cells were cultured at 37°C with 5% CO_2 for 9 days. At day 10, the numbers of colonies was counted and one-fourth of the total colonies were randomly picked, cytospun, and stained with Hemacolor (Merck) for colony scoring.

For M-CSF treatment, the prepared bone marrow cells were seeded into Methocult supplemented with the cytokines indicated above in addition to 10 ng/ml M-CSF (Peprotech) and assayed as described above. All cultures were performed in duplicate.

2.14 Statistical analysis

Statistical analysis was performed with Microsoft Excel or GraphPad Prism 4 (GraphPad Software, La Jolla, CA, U.S.A.). Statistical tests included unpaired or paired Student's t tests and ordinary one-way ANOVA followed by Tukey's multiple comparisons tests. For non-parametric data sets, the statistical significances were examined using Kruskal Wallis H tests followed by Steel-Dwass tests. Survival data were analyzed by a Kaplan-Meier method and log-rank test. A value of $P < 0.05$ was considered to be statistically significant.

2.15 Determination of the transgene integration site

2.15.1 Whole genome sequence of T-bet transgenic mouse

Genomic DNA of the T-bet transgenic mouse was extracted from liver using a QIAGEN QIAmp DNA Micro kit (Qiagen Sciences, Germantown, MD). A total of 10 mg of genomic DNA was sheared using the Covaris S-series (Woburn, MA), and the sheared DNA was used to generate sequencing libraries following the standard Illumina protocols for Mate-pair Library Prep Kit v2 (Illumina, San Diego, CA). Sequencing was performed on an Illumina HiSeq 2000 sequencer (Illumina), using the TruSeq Paired-End Cluster Kit v3 (Illumina) and the TruSeq SBS HS Kit v3 (Illumina), generating 2 × 100 bp reads. Image analysis and base calling was done using the HiSeq Control Software version 1.4.8 and Consensus Assessment of Sequence and Variation (CASAVA) v1.8.1.

2.15.2 Data analysis

Mouse reference genome (mm9) and human reference genome (hg19) was obtained from the Build 37 assembly by National Center for Biotechnology Information (NCBI). Transgene sequence reference was produced manually with combination of upstream sequence of human CD2 gene (chr1:117,292,085-117,297,268, hg19), mouse Tbx21 coding sequence (NM_019507.2) and downstream sequence of human CD2 gene (chr1:117,311,852-117,317,352, hg19). Sequence reads from HiSeq 2000 were mapped to each genome reference sequence using Burrows-Wheeler Aligner version 0.5.9 (52). We extracted discordant pair reads with one mapped on mm9 reference and the other mapped on the transgene sequence reference described above.

2.15.3 Confirmation of the breakpoint by direct sequence

PCR was performed using primer pairs described in Table 1. PCR products were subjected to the direct sequence using the BigDye Terminator v.1.1 Cycle Sequencing Kit (LifeTechnologies) on an ABI PRISM 3130 Genetic Analyzer (LifeTechnologies).

2.15.4 Results

A total of 473,766,898 reads was generated by HiSeq2000 sequence, and 286,549,897 reads (60.4%) were mapped on the reference genomes. The average coverage was 10.5 for mm9 reference. We obtained 68 discordant pair reads, and among them, we selected 13 discordant pair reads with multiple hits (≥5). All of these 13 discordant pairs were located on chromosome 11 of mm9 reference. Direct sequence was performed to identify exact locations of the breakpoints. The sequence produced by primer pairs, chr11L and 11R, is shown in Figure 3 B and Table 2. Figure 3 A shows the schematic representation of the transgene on chromosome 11 of mouse genome reference mm9. We identified the transgenes were inserted between chr11: 13,474,589 and chr11: 13,474,610, and 19 kb deletion between chr11: 13,454,172 and chr11: 13,473,547. We confirmed no endogenous genes in this region.

Chapter 3: Results

3.1 Aged *CD2-T-bet*$^{tg/tg}$ mice spontaneously develop PAP-like disease

Accumulating evidence suggests that aberrant T-bet expression is often coupled with various inflammatory diseases. To gain insight into the special link between T-bet and inflammation, we generated CD2-T-bet transgenic mouse (CD2-T-bet tg) lines in accordance with previous report (51). The expressions of T-bet were approximately 15 and 5 times higher in the lungs of *T-bet*$^{tg/tg}$ and *T-bet*$^{tg/wt}$ mice than that in wild-type (WT) mice, respectively (Figure 1 A). Of note, starting from about 20 weeks of age, more than 80% of *T-bet*$^{tg/tg}$ mice died with pulmonary pathology under specific pathogen-free conditions, whereas all *T-bet*$^{tg/wt}$ and WT mice survived within the observation period of over 2 years (Figure 1 B). In addition to lymphoid hyperplasia around airways and veins, we observed the presence of acellular eosinophilic material and a severe infiltration of inflammatory cells in the alveolar space of the moribund mice (Figure 1 C). As we further investigated the histology of lung tissues, we observed that the acellular material that filled the distal air spaces of the *T-bet*$^{tg/tg}$ mice was positive with the Periodic acid-Schiff (PAS) staining (Figure 1 D). Immunohistochemical analysis of the lung tissues showed that the material was also positive for surfactant protein-A (SP-A) antibody stainings, collectively indicating abnormal surfactant accumulation in the alveolar spaces (Figure 1 D). No pathological findings were observed in other organs such as the spleen, liver, kidney, and small intestine of moribund mice (Figure 2). Remarkably, the collected bronchoalveolar lavage fluid (BALF) of *T-bet*$^{tg/tg}$ mice looked considerably cloudier than those of their siblings (*T-bet*$^{tg/wt}$ and WT), which is a characteristic of BAL samples obtained from PAP patients (Figure 1 E). Cytological examinations revealed the existence of foamy macrophages in the collected BALF samples (Figure 1F). Expression analysis with mRNAs from the lungs demonstrated that SP-A expressions were comparable between the groups, indicating that surfactant production did not become increased (Figure 5A).

Altogether, these results strongly suggest that aged *T-bet*$^{tg/tg}$ mice spontaneously developed a pulmonary syndrome resembling human PAP.

3.2 The development of PAP in *T-bet*$^{tg/tg}$ mice depends on the transgene

Since the PAP development was observed in *T-bet*$^{tg/tg}$ mice, but not in *T-bet*$^{tg/wt}$ mice, we suspected that the phenotype occurred due to a gene disruption during the integration of the transgene into the genome. Moreover, it has been difficult to determine the genotype of each mouse, as we did not know the integration site of the transgene in the genome. For example, we had to backcross each of the pups to a wild-type mouse to distinguish *T-bet*$^{tg/wt}$ from *T-bet*$^{tg/tg}$. To address the issue, we performed a transgene integration analysis using the genomic DNA obtained from a *T-bet*$^{tg/wt}$ mouse and revealed that the transgene was integrated in an intergenic region on the chromosome 11, indicating that no genes were disrupted in the PAP mice (Figure 3 A). Utilizing the information, we were able to design a PCR primer pair for the determination of the genotype of each mouse with DNAs prepared from tail tips (Figure 3 B and C). In addition, we observed PAP development in *T-bet*$^{tg/tg}$ mice from other transgenic mouse line, providing further evidence that PAP was induced by T-bet overexpression (Figure 4). These results indicate that *T-bet*$^{tg/tg}$ mice developed PAP independently of a protein-coding gene and a non-coding RNA deficiencies, but rather by the mechanism that is initiated by T-bet over expression in T cells.

3.3 *T-bet*$^{tg/tg}$ mice develop PAP without an acquired GM-CSF-PU.1 axis defect

To assess if the observed PAP development is due to an acquired GM-CSF signaling attenuation, as some secondary PAP development associate with it, we analyzed the expressions of GM-CSF signaling-related genes using mRNAs extracted from the lung tissues and alveolar macrophages. A significant elevation of GM-CSF expression in the lung

of *T-bet*$^{tg/tg}$ mice was observed relative to their controls (Figure 5 B). The expressions of the beta chain of GM-CSF receptor (GM-CSFRβc), which is involved in its signal transduction, was also up-regulated in *T-bet*$^{tg/tg}$ macrophages than in those of other genotypes, while expressions of the alpha chain (GM-CSFRα) was lower in both *T-bet*$^{tg/tg}$ and *T-bet*$^{tg/wt}$ macrophages (Figure 5 C). The transcription factor PU.1 is a downstream molecule of GM-CSF signaling and mediates GM-CSF-dependent terminal differentiation of alveolar macrophages. In GM-CSF-deficient mice, a marked reduction of PU.1 expression causes an impairment of macrophage differentiation and PAP development (27). However, the expression level of PU.1 in *T-bet*$^{tg/tg}$ macrophages was comparable to that of WT (Figure 5 D). Since down regulation of *GM-CSFRA* expression and elevation of sera and BALF GM-CSF in hereditary PAP patients has been reported, we considered the possibility that GM-CSF protein concentration was also elevated in BALFs and sera of *T-bet*$^{tg/tg}$ mice. Nonetheless, we did not detect GM-CSF proteins in neither BALFs nor sera of WT, *T-bet*$^{tg/wt}$, and *T-bet*$^{tg/tg}$ mice with cytometric beads array (CBA) (Data not shown). Collectively, these results demonstrate that development of PAP in *T-bet*$^{tg/tg}$ mice is independent of acquired GM-CSF signaling defects.

3.4 Aberrant overexpression of T-bet in lymphocytes initiates PAP development

The results so far suggest that the aged *T-bet*$^{tg/tg}$ mice develop PAP-like disease due to previously unknown mechanisms. We therefore considered the possibility that the T-bet overexpressing lymphocytes alone are able to initiate PAP-like disease. To assess the question, we examined whether the lymphocytes aberrantly expressing T-bet could induce the development of the PAP-like disease in lymphocyte-deficient recipients. Specifically, we transplanted the lymphocytes expressing CD45.2 from the spleens of the moribund mice and the controls (*T-bet*$^{tg/wt}$ and WT) into CD45.1-*Rag2*$^{-/-}$ recipients (Figure 6). Lung H&E

sections of the recipients transplanted with *T-bet*$^{tg/tg}$ splenocytes (t*T-bet*$^{tg/tg}$) demonstrated massive infiltration of hematopoietic cells into and accumulation of acellular materials in the alveolar spaces (Figures 6 B). Although inflammatory cells had infiltrated slightly, PAP did not develop in recipients transplanted with *T-bet*$^{tg/wt}$ splenocytes (t*T-bet*$^{tg/wt}$) (Figures 6 B). We also confirmed long-term engraftment of the donor cells in the recipient spleens (Figure 6 C). These results clearly indicate that the Rag2-deficient recipients developed the disease phenotype recapitulating the core features of the disease developed in the primary PAP mice and hence suggest that aberrant overexpression of T-bet in lymphocytes alone is sufficient to initiate PAP-like disease development in mice.

3.5 T-bet overexpressing T cells are sufficient to induce PAP development

To further examine the ability of T-bet-overexpressing T cells from *T-bet*$^{tg/tg}$ mice for PAP development, we performed adoptive transfer of CD3ε^{+} T cells obtained from *T-bet*$^{tg/tg}$ and WT mice into *Rag2*$^{-/-}$ recipients (Figure 7 A). We choose *Rag2*$^{-/-}$ mice as recipients so as to investigate if B cells and/or autoantibodies were required for the development of PAP. Flowcytometric analysis of donor T cells revealed that more than 95% of the transferred cells were CD3ε^{+} T cells, leaving less than 1% of it B220^{+} cells (Figure 7 B). Monthly peripheral blood analysis showed an increase in WBC density of recipients received *T-bet*$^{tg/tg}$ T cells compared to that of WT recipients, whereas the frequency of PB CD3ε^{+} cells was comparable to that of WT (Figure 7 C). We also confirmed a few B220^{+} cells in their PB (less than 0.3%) throughout the experimental period. Moreover, compared to the control group, increases in the numbers of PB Ly6C^{High} inflammatory monocytes and neutrophils were observed in recipients harboring *T-bet*$^{tg/tg}$ T cells starting from 12 weeks after transplantation (Figure 7 D). Histological analyses of moribund mice revealed that they developed PAP-like disease with an accumulation eosinophilic material that stained positive for PAS surfactant in the

alveoli (Figure 7 E and F). Flowcytometric analysis with their splenocytes demonstrated no or few engraftment of $B220^{+}$ cells in the spleens of the moribund recipients. These results indicate that *T-bet*$^{tg/tg}$ T cells are sufficient to initiate PAP-like disease development without significant contribution of B cells.

3.6 Expression levels of genes associated with immune and inflammatory responses are selectively elevated in the lung of PAP mice

To uncover potential mechanisms underlying the observed PAP-like phenotype, we performed a microarray analysis using lung mRNAs from T-bet tg mice. We detected 653 genes whose expression changed by at least 10-fold between genotypes. Consistent with the histological findings, clustering and gene ontology analyses revealed that genes related to inflammatory and immune responses were particularly enriched in *T-bet*$^{tg/tg}$ lungs (Figure 8A). In addition, qPCR analysis confirmed upregulation of IFN-γ and TNF expressions selectively in *T-bet*$^{tg/tg}$ samples (Figure 8B). These results indicate selective induction of aberrant inflammatory responses in the lungs of *T-bet*$^{tg/tg}$ mice.

3.7 Proinflammatory cytokine production is enhanced in the lungs of PAP mice

Massive infiltration of inflammatory cells and upregulation of Th1 cytokine gene expressions in the lungs of *T-bet*$^{tg/tg}$ mice suggested that their lungs are under proinflammatory condition. To address the possibility, we quantified inflammatory cytokines in the BAL fluids of *T-bet*$^{tg/tg}$, *T-bet*$^{tg/wt}$, and WT mice at 30-50 week of age. The concentrations of proinflammatory cytokines including IFN-γ, TNF, and IL-6 were markedly elevated in the BAL fluids of *T-bet*$^{tg/tg}$ mice with PAP-like phenotype compared with those in the BAL fluids of other genotypes (Figure 9 A-C). We also observed a substantial increase of BAL fluids monocyte chemoattractant protein-1 (MCP-1) concentration, as previously described in PAP patients

(Figure 9 D) (53). However, the concentrations of IL-12p70, IL-10, and IL-4, were comparable between the genotypes. Moreover, we observed that IL-2, and IL-17A were under the detection levels. These results indicate that proinflammatory cytokines and CCR2 ligand were extensively produced only in the lung of *T-bet*$^{tg/tg}$ mice, suggesting its involvement in the development of PAP in these mice.

3.8 Subpopulations of BAL cell are altered in the lungs of PAP mice

The results of cytokine quantifications have raised a question of what types of cells in the alveoli of the PAP mice are responsible for the productions of these cytokines. To address the question, we further analyzed the constituents of BAL cells from mice of each genotype. We first counted the numbers of total cells, macrophages/monocytes, neutrophils, and lymphocytes in BAL fluids. The numbers of inflammatory cells, including lymphocytes, neutrophils, and most prominently macrophages/monocytes, were significantly higher in the BALF of *T-bet*$^{tg/tg}$ mice than those of other genotypes (Figures. 10 A and B). To gain more information on subpopulation of each leukocyte subset, we also analyzed subpopulations of BAL-recovered cells by flow cytometry. In WT mice, most of BAL-recovered cells were Autofluorescence (AF)$^{+}$ and CD11c^{+} alveolar macrophages (Figure 10 C) (54). However, severe reductions of the alveolar macrophage population were observed in *T-bet*$^{tg/tg}$ lungs (Figure 10 C). Instead of alveolar macrophages, we found that AF^{+}, F4/80^{low}, CD11b^{+} bone marrow (BM)-derived macrophages (55) as well as T cells had infiltrated into *T-bet*$^{tg/tg}$ lungs (Figures 10 D and E). A population that did not fit into both populations with AF^{+} also emerged in the BAL samples (Figure 10 D). Although a slight reduction of the alveolar macrophage population was observed in *T-bet*$^{tg/wt}$ mice, BM-derived macrophages did not infiltrate into their alveoli (Figure 10 E). As phenotypic changes often associated with functional alternation, we further performed functional assay and expression analysis of

genes known to take roles in PAP development. Phagocytic assay demonstrated a significant reduction of phagocytic ability of BAL cells from *T-bet*$^{tg/tg}$ mice (Figure 10 F). Gene expressions of *Pparg* and *Abcg1*, which were known to induce PAP when they are deleted in mice, were selectively down regulated in AF^{+} BAL cells from *T-bet*$^{tg/tg}$ with PAP phenotypes (Figure 10 G). These findings indicate that changes in immunophenotype and functional impairment essential to lipid handlings may involve in the development of PAP in *T-bet*$^{tg/tg}$ mice.

3.9 Increased numbers of inflammatory monocytes numbers in the circulation of PAP mice

Although we have identified some of the features that are unique to *T-bet*$^{tg/tg}$ mice with PAP-like disease, detailed cellular and molecular events during the disease progression remains unknown. Therefore, to gain more insights into the disease development, we performed a series of peripheral blood examinations using the T-bet tg mice at 25-35 weeks of age, including both moribund and relatively healthier *T-bet*$^{tg/tg}$ mice, and *Rag2*$^{-/-}$ recipients carrying the splenocytes of the T-bet tg mice (Figure 11). Inflammatory monocytes are known as the precursor of BM macrophages, also known as inflammatory macrophages, and hence actively participate in initiating the clearance of the local inflammatory stimuli. The concentrations of white blood cells were not significantly altered in both *T-bet*$^{tg/tg}$ and *T-bet*$^{tg/wt}$, although those of *T-bet*$^{tg/tg}$ mice showed relatively higher numbers (Figure 11 A). To investigate the composition of white blood cells in their blood, we further performed flow cytometric analyses (Figure 11 B). Among the white blood cells, CD11b^{+} myeloid cell numbers were higher in both *T-bet*$^{tg/tg}$ and *T-bet*$^{tg/wt}$ peripheral blood (PB) relative to WT mice (Figure 11 C). Of note, we observed higher numbers of Ly6C^{High}, Gr-1^{Mid} inflammatory monocytes in the blood of *T-bet*$^{tg/tg}$ mice relative to those of *T-bet*$^{tg/wt}$ and WT mice (Figure

11 D). Importantly, the high blood inflammatory monocyte numbers was associated with PAP development. On the contrary, the numbers of neutrophils in the PB from *T-bet*$^{tg/tg}$ mice was not significantly elevated compared to the controls, although some *T-bet*$^{tg/tg}$ mice showed increased neutrophil concentrations (Figure 11 E). The periodical measurements of the complete blood counts from the *Rag2*$^{-/-}$ recipients showed that white blood cell (WBC) counts of *tT-bet*$^{tg/tg}$ mice gradually increased (Figure 11 F). In parallel with the increase in WBC counts, flow cytometric analyses of the PB revealed that the concentrations of the recipient-driven (CD45.1^{+}) inflammatory monocytes progressively increased in t*T-bet*$^{tg/tg}$ mice, whereas those of recipient-driven neutrophil in the PB of *tT-bet*$^{tg/tg}$ mice remained unchanged and were comparable to those of controls (Figures 11 G and H). These results indicate that the development of PAP in the *T-bet*$^{tg/tg}$ mice is associated with increasing number of BM-derived inflammatory monocytes in the PB.

3.10 The bone marrow hematopoietic stem/progenitor cells from *T-bet*$^{tg/tg}$ mice acquire monocytic differentiation impairment

The results described thus far together with the finding that the half life of circulating Ly6C^{+} monocyte is about one day (56) have suggest that monocytic differentiation of the bone marrow hematopoietic stem/progenitor cells is affected by aberrant long-term T-bet overexpression in T cells. To assess this hypothesis, we explored the effects on the differentiation of hematopoietic stem/progenitor cells by performing colony-forming cell (CFC) assays using 25-30 week-old mice (Figure 12 A). The whole bone marrow cells (WBMCs) in the femur of *T-bet*$^{tg/tg}$ mice generated higher numbers of colony-forming unit (CFU) (Figure 12 C, the left column), whereas their cell numbers were comparable to those of controls (Figure 12 B). Identification of the types of each colony showed that the numbers of each CFU (CFU-M, GM, GEMM, and BFU-E) remained unchanged, suggesting that the

differentiation potentials remained unchanged (Figure 12 C, right 5 columns). Strikingly, compared with *T-bet*$^{tg/wt}$ and WT mice, we noticed that a significant number of colonies derived from *T-bet*$^{tg/tg}$ WBMCs contained a considerable number of morphologically immature monocytic cells (Figures 12 D and E). The number of CFUs with such cells from *T-bet*$^{tg/wt}$ WBMCs was significantly higher than that of wild type (Figure 12 F). The findings demonstrate that the bone marrow hematopoietic stem/progenitor cells (HSPCs) from PAP mice acquire an impairment of monocytic differentiation while producing increased numbers of progenitor cells.

To study if the observed immature cells were monocytic lineage cells, we examined the effects of macrophage-colony stimulating factor (M-CSF) on the dysregulated myeloid differentiation of HSPCs from the PAP mice. The development of monocytic lineage cells descends from HSCs with discrete intermediate progenitor cells, including monocyte/dendritic cell progenitors (MDPs) expressing CD115, the receptor for M-CSF (57). Addition of M-CSF into the culture system as described above resulted in a significant reduction of the number of CFU including immature monocytic cells (Figure 12 G). This result implies that the monocytic differentiation impairment is either reversible or promoted by the addition of the lineage-specific cytokine, M-CSF and adds another evidence that monocytic differentiation of the BM HSPCs was intrinsically impaired in PAP mice.

An increase in the number of CFU from *in vitro* CFC assays with *T-bet*$^{tg/tg}$ BMCs has indicated the possibility that the numbers of subsets of HSPCs in their BMs are increased. To assess the possibility, we performed flowcytometric analysis using BMCs of 30-50 week-old mice and investigated the frequencies of subsets of HSPCs. However, we did not find any subsets, including monocyte/dendritic cell progenitors (MDPs), that were significantly increased in *T-bet*$^{tg/tg}$ BM compared to those of the controls, whereas that of long-term hematopoietic stem cells (HSCs) (defined immunophenotypically as Lineage markers^{-}/c-

kit^{+}/Sca-1^{+}/CD34^{-}/CD150^{+}) was slightly increased (Figure 13). The result suggests that the numbers of HSPCs were not significantly affected in *T-bet*$^{tg/tg}$ mice.

Chapter 4: Discussion

4.1 Summary of the findings

The pathogenesis of acquired PAP without GM-CSF signaling defects has long been unknown. We demonstrated here a novel mechanism by which acquired PAP development is initiated in mice independently of GM-CSF defects. We further provided pathophysiological features that were unique to PAP-like disease development in this mouse model.

4.2 T-bet overexpression as a novel pathogenesis of acquired PAP

We demonstrated the development of PAP in aged *CD2-T-bet*$^{tg/tg}$ mice. All of the pathological features displayed in the moribund *CD2-T-bet*$^{tg/tg}$ mice represent the main clinical and laboratory features of PAP and the phenotypes of GM-CSF signaling deficient mice, which spontaneously develop PAP. Expression analyses of GM-CSF signaling molecules revealed that the *CD2-T-bet*$^{tg/tg}$ mice develop PAP not due to its down-regulation in the lung. Subsequent *in vivo* studies with the mice indicated that our transgenic mice develop PAP-like disease secondary to aberrant T-bet overexpression in T cells, but not primarily through an alveolar macrophage-intrinsic defect, including an acquired GM-CSF signaling attenuation mediated by PU.1. To date, there have been a few studies reporting the development of secondary PAP disease models (10). One of them has shown that the development of secondary PAP in *scid/scid* mice, presumably recapitulating secondary PAP patients with immunodeficiency, although the mechanism has not been identified (58). Besides, a recent study has shown that a transcription factor, Bach2, also plays critical role in pulmonary surfactant homeostasis and its deficiency leads to PAP development with an impaired macrophage activation ability for wound healing (M2 activation) in mice (59). On the contrary, the present model develops PAP under aberrant T cell activation by T-bet accompanied by upregulation of *Bach2* expression levels in lung macrophages. Intriguingly,

previous studies have demonstrated upregulation of T-bet expression in several hematological malignancies, which are the most common underlying diseases of secondary PAP (60, 61). Nonetheless, studies using BAL samples from autoimmune and secondary PAP patients, presumably suffered from MDS, are absolutely necessary to propose that T-bet overexpression in T cells are an underlying mechanism of secondary PAP.

4.3 T-bet overexpressing T cells can initiate PAP development with minimum contribution of B cells

We also demonstrated that T cells overexpressing T-bet plays pivotal roles in inducing PAP-like phenotype in *Rag2*$^{-/-}$ mice, which lack both mature T and B cells (62), through adoptive transfer of T cells. Although previous studies have shown that the transgene expression used in the current study is restricted to T cell lineages, there remains the possibility that T cells in the mice aberrantly provoke autoantibody productions (49, 63). Nonetheless, the results indicated that only the T cells were sufficient to trigger PAP development without prior existence of mature B cells. In accordance with the finding, we observed no PAP development in *hCD2-T-bet*$^{tg/tg}$ on Balb/c background. The next question that follows is which T cell subset (s) is actively participated in the disease development. Since a previous study has demonstrated both $CD4^+$ and $CD8^+$ T cells overexpress T-bet in the current system, it is currently unknown which subset is involved in PAP development. In addition, T-bet expression is also crucial to mount the functions and development of non-conventional T cells, including invariant natural killer T cells and γδ T cells (64, 65). Adoptive transfer experiments with those fractionated T cell subsets will address the question.

4.4 Reorganization of macrophage subpopulations and PAP development

Our results indicated that reorganization of macrophage subpopulation in the alveoli is

involved in PAP development in the mice. Recent studies have demonstrated that not all macrophages in tissues do not originate from hematopoietic stem cells through bone marrow progenitors, but rather subsets of tissue macrophages substantially develop from embryonic progenitors in the yolk sac and can self-renew to maintain its populations throughout the adult life (66). Recent data also suggest that inflammatory monocyte-derived populations can be immunophenotypically and functionally discriminated from the yolk sac-derived populations in tissues (55, 67-70). In particular, consistent with our observations regarding BAL samples obtained from WT mice, alveolar macrophages exclusively comprised adult BAL cell population in mice under homeostasis (71). However, we observed a severe reduction of alveolar macrophage population in *T-bet*$^{tg/tg}$ BAL samples. In addition, we found appearance of a macrophage population that coincides with the surface marker profile of monocyte-derived BM-macrophages. It is worthwhile to mention that those immunophenotypical differences were the consequence of alveolar macrophages with altered surface marker expressions. The alveolar macrophages not only play a central role in pulmonary lipid homeostasis, but also represent the first line of defense in the alveoli against invading pathogens and inhaled microbes and its absence results in reduced clearance during infections (72, 73). In persistent inflammatory conditions, however, these alveolar macrophages receive aids from BM-macrophages, also known as inflammatory or M1 activated macrophages, with increased microbicidal activities including augmented NOS, TNF, and IL-6 productions (74-76). Similarly, we observed marked increases in proinflammatory cytokine concentrations, such as TNF and IL-6 in the lung of the mice. Importantly, a study using bone marrow transplantation has shown that the development of PAP in GM-CSF-deficient mice critically depends on impaired turnover of host-derived tissue macrophages, but not on impaired replacement by monocytes originated from donor-derived hematopoietic stem cells both in homeostatic and challenge conditions, indicating

that the functions of alveolar macrophages cannot be compensated by BM-derived macrophages (77). Those previous observations well fit into the results from our functional assays showing reduction of phagocytic ability and gene expressions essential to surfactant catabolism. Importantly, a previous study also have shown that PPARγ regulates resolution phase during inflammation and maintains integrity of alveolar macrophages (78). These observations dovetail with our findings that phenotypical and functional changes in the macrophage subpopulations in the lung induced by T-bet overexpressing T cells lead to accumulation of alveolar surfactant in *T-bet*$^{tg/tg}$ mice.

4.5 Involvement of BM-derived cells in PAP development

We were able to provide further evidence that BM macrophages are involved in the disease progression. We found especially the association between the development of PAP and a progressive increase in circulating inflammatory monocytes. Moreover, we also observed a considerable increase in the concentration of MCP-1 in the lung of PAP mice. Several lines of evidence suggest that CCR2/MCP-1 interactions significantly contribute to monocyte, macrophage and T cell recruitment to the sites of inflammation (79, 80). These findings suggest that the infiltration of the circulating inflammatory monocytes into the lung in the PAP mice may be mediated by the interaction between CCR2, a receptor for MCP-1, and MCP-1. Identifying the mechanisms by which the T-bet overexpressing T cells as well as inflammatory monocytes specifically infiltrate into the lung is intriguing and requires further investigation.

4.6 An acquired dysregulation of hematopoiesis of myeloid cells

We demonstrated both *in vitro* and *in vivo* an acquired dysregulation of bone marrow hematopoiesis in *T-bet*$^{tg/tg}$ mice. These findings are in part in line with recent reports from

the fields of microbial infections and chronic inflammatory diseases that hematopoietic stem/progenitor cells are directly stimulated by environmental cues, including proinflammatory cytokines (81). For example, Griseri *et al.* has shown recently that inflammatory cytokines mediates dysregulated hematopoiesis in IL-23-dependent colitis at hematopoietic stem cell level (82). Of note, we found, unexpectedly, that the monocytic differentiation became intrinsically impaired at *CD2-T-bet*$^{tg/tg}$ bone marrow HSPC level, although its underlying mechanisms regulating these effects are currently unknown. The relationship between T-bet overexprssion and bone marrow failure has been demonstrated in patients with aplastic anemia and myelodysplastic syndrome (47, 83-86). In this regard, activated $CD8^+$ T cells- and IFN-γ-mediated reduction of bone marrow stem and progenitor cells have been identified as a cellular mechanism (87, 88). Nevertheless, we did not observe definitive evidence for the development of aplastic anemia and myelodysplasia i*n vivo*. Therefore, results from CFC assays and PB analysis suggest that differentiation programs from monocytes to macrophages were disrupted due to T-bet-overexpressing T cells, which lead to the reduction of functionally mature alveolar macrophage population as a whole.

4.7 Possible signaling pathways

Results showing increased PB inflammatory monocytes by peripheral blood examinations, unchanged macrophage/dendritic cell progenitor frequency by flowcytometry, and profound increase in immature monocytic colonies by CFC-assays strongly suggest that differentiation of monocyte/macrophage lineage in *T-bet*$^{tg/tg}$ mice is impaired at the stage where inflammatory monocytes differentiate into macrophages. In addition, the observation that the impaired monocyte/macrophage maturation was greatly ameliorated by the addition of M-CSF, the critical regulator for the lineage, suggest the pathway may have been dysregulated. Nevertheless, there still remains the possibility that other cytokine signaling, along with GM-

CSF or G-CSF signalings, may play roles in the pathogenesis. Although we have tried to perform intracellular flowcytometric analyses for pStat5 and pAkt, we found the autofluorescence intrinsic to alveolar macrophages leaks to most of the channels during flowcytometric analysis, making it difficult to detect otherwise small changes. In addition to the detection problem inherited to flowcytometry, it turn out that the number of total BAL cells that we can obtain was suboptimal (1-5 x 10^5 cells/mouse) for both a flowcytometry and a western blot analyses. Although it has been of great interest for us, to the best of our knowledge, answering the questions requires further technical advance. Previous study has shown an increased IFNγ signaling responses when the expression of PPARγ in alveolar macrophages is suppressed (89). Taking those studies into an account, our results indicate that IFNγ produced by T-bet may directly involve in the functional impairment of lung macrophages by suppressing the expression of PPARγ, thereby inhibiting its lipid handing as well as integrity.

Chapter 5: Conclusion

The current study unveils an unexpected link between T-bet overexpression in T cells and PAP development, a disorder of pulmonary surfactant homeostasis. Previous studies identified disruption of GM-CSF signaling as a pathogenesis of PAP, but other PAP pathogenesis has not been explored. Here, we demonstrate that T-bet overexpression in T cells can induce the development of PAP-like disease in mice. We also identify several pathophysiological features that are unique to the disease development. Collectively, tshe present model may replicate certain aspects of the disease progression displayed in patients with PAP secondary to hematological disorders. To date, the pathogenesis of secondary PAP, which occurs independently of GM-CSF signaling defects, is poorly understood. Studies with clinical samples are currently undergoing to evaluate physiological relevance of the findings. Taken together, the current study may provide a new insight into our understanding of the pathogenesis of acquired PAP.

Chapter 6: References

1. Trapnell, B. C., J. A. Whitsett, and K. Nakata. 2003. Pulmonary alveolar proteinosis. *N Engl J Med* 349: 2527–2539.

2. Rosen, S. H., B. Castleman, A. A. Liebow, F. M. Enzinger, and R. T. N. Hunt. 1958. Pulmonary Alveolar Proteinosis. *N Engl J Med* 258: 1123–1142.

3. Maygarden, S. J., M. V. Iacocca, W. K. Funkhouser, and D. B. Novotny. 2001. Pulmonary alveolar proteinosis: a spectrum of cytologic, histochemical, and ultrastructural findings in bronchoalveolar lavage fluid. *Diagn. Cytopathol.* 24: 389–395.

4. Wang, B. M., E. J. Stern, R. A. Schmidt, and D. J. Pierson. 1997. Diagnosing pulmonary alveolar proteinosis. A review and an update. *Chest* 111: 460–466.

5. Seymour, J. F., and J. J. Presneill. 2002. Pulmonary alveolar proteinosis: progress in the first 44 years. *Am J Respir Crit Care Med* 166: 215–235.

6. Ben-Dov, I., Y. Kishinevski, J. Roznman, A. Soliman, H. Bishara, E. Zelligson, J. Grief, A. Mazar, M. Perelman, R. Vishnizer, and D. Weiler-Ravel. 1999. Pulmonary alveolar proteinosis in Israel: ethnic clustering. *Isr. Med. Assoc. J.* 1: 75–78.

7. Prakash, U. B., S. S. Barham, H. A. Carpenter, D. E. Dines, and H. M. Marsh. 1987. Pulmonary alveolar phospholipoproteinosis: experience with 34 cases and a review. *Mayo Clin. Proc.* 62: 499–518.

8. deMello, D. E., and Z. Lin. 2001. Pulmonary Alveolar Proteinosis: A Review. *Fetal Pediatr Pathol* 20: 413–432.

9. Goldstein, L. S., M. S. Kavuru, P. Curtis-McCarthy, H. A. Christie, C. Farver, and J. K. Stoller. 1998. Pulmonary alveolar proteinosis: clinical features and outcomes. *Chest* 114: 1357–1362.

10. Carey, B., and B. C. Trapnell. 2010. The molecular basis of pulmonary alveolar proteinosis. *Clin. Immunol.* 135: 223–235.

11. Nogee, L. M. 2006. Genetics of pediatric interstitial lung disease. *Current Opinion in Pediatrics* 18: 287–292.

12. Nogee, L. M. 2004. Genetic mechanisms of surfactant deficiency. *Biol. Neonate* 85: 314–318.

13. Dranoff, G., A. D. Crawford, M. Sadelain, B. Ream, A. Rashid, R. T. Bronson, G. R. Dickersin, C. J. Bachurski, E. L. Mark, and J. A. Whitsett. 1994. Involvement of granulocyte-macrophage colony-stimulating factor in pulmonary homeostasis. *Science* 264: 713–716.

14. Stanley, E., G. J. Lieschke, D. Grail, D. Metcalf, G. Hodgson, J. A. Gall, D. W. Maher, J. Cebon, V. Sinickas, and A. R. Dunn. 1994. Granulocyte/macrophage colony-stimulating factor-deficient mice show no major perturbation of hematopoiesis but develop a characteristic pulmonary pathology. *Proc. Natl. Acad. Sci. U.S.A.* 91: 5592–5596.

15. Uchida, K., K. Nakata, B. C. Trapnell, T. Terakawa, E. Hamano, A. Mikami, I. Matsushita, J. F. Seymour, M. Oh-Eda, I. Ishige, Y. Eishi, T. Kitamura, Y. Yamada, K. Hanaoka, and N. Keicho. 2004. High-affinity autoantibodies specifically eliminate granulocyte-macrophage colony-stimulating factor activity in the lungs of patients with idiopathic pulmonary alveolar proteinosis. *Blood* 103: 1089–1098.

16. Martinez-Moczygemba, M., M. L. Doan, O. Elidemir, L. L. Fan, S. W. Cheung, J. T. Lei, J. P. Moore, G. Tavana, L. R. Lewis, Y. Zhu, D. M. Muzny, R. A. Gibbs, and D. P. Huston. 2008. Pulmonary alveolar proteinosis caused by deletion of the GM-CSFRalpha gene in the X chromosome pseudoautosomal region 1. *J. Exp. Med.* 205: 2711–2716.

17. Suzuki, T., T. Sakagami, L. R. Young, B. C. Carey, R. E. Wood, M. Luisetti, S. E. Wert, B. K. Rubin, K. Kevill, C. Chalk, J. A. Whitsett, C. Stevens, L. M. Nogee, I. Campo, and B. C. Trapnell. 2010. Hereditary pulmonary alveolar proteinosis: pathogenesis, presentation, diagnosis, and therapy. *Am J Respir Crit Care Med* 182: 1292–1304.

18. Suzuki, T., T. Sakagami, B. K. Rubin, L. M. Nogee, R. E. Wood, S. L. Zimmerman, T. Smolarek, M. K. Dishop, S. E. Wert, J. A. Whitsett, G. Grabowski, B. C. Carey, C. Stevens, J. C. M. van der Loo, and B. C. Trapnell. 2008. Familial pulmonary alveolar proteinosis caused by mutations in CSF2RA. *J. Exp. Med.* 205: 2703–2710.

19. Kitamura, T., N. Tanaka, J. Watanabe, Uchida, S. Kanegasaki, Y. Yamada, and K. Nakata. 1999. Idiopathic pulmonary alveolar proteinosis as an autoimmune disease with neutralizing antibody against granulocyte/macrophage colony-stimulating factor. *J. Exp. Med.* 190: 875–880.

20. Trapnell, B. C., and J. A. Whitsett. 2002. GM-CSF regulates pulmonary surfactant homeostasis and alveolar macrophage-mediated innate host defense. *Annu. Rev. Physiol.* 64: 775–802.

21. Hansen, G., T. R. Hercus, B. J. McClure, F. C. Stomski, M. Dottore, J. Powell, H. Ramshaw, J. M. Woodcock, Y. Xu, M. Guthridge, W. J. McKinstry, A. F. Lopez, and M. W. Parker. 2008. The Structure of the GM-CSF Receptor Complex Reveals a Distinct Mode of Cytokine Receptor Activation. *Cell* 134: 496–507.

22. Hercus, T. R., D. Thomas, M. A. Guthridge, P. G. Ekert, J. King-Scott, M. W. Parker, and A. F. Lopez. 2009. The granulocyte-macrophage colony-stimulating factor receptor: linking its structure to cell signaling and its role in disease. *Blood* 114: 1289–1298.

23. Watanabe, S., T. Itoh, and K. Arai. 1996. Roles of JAK kinases in human GM-CSF receptor signal transduction. *J. Allergy Clin. Immunol.* 98: S183–91.

24. Hackenmiller, R., J. Kim, R. A. Feldman, and M. C. Simon. 2000. Abnormal Stat activation, hematopoietic homeostasis, and innate immunity in c-fes-/- mice. *Immunity* 13: 397–407.

25. D'Andrea, R. J., and T. J. Gonda. 2000. A model for assembly and activation of the GM-CSF, IL-3 and IL-5 receptors: insights from activated mutants of the common beta subunit. *Experimental Hematology* 28: 231–243.

26. Shearer, W. T., L. J. Rosenwasser, B. S. Bochner, M. Martinez-Moczygemba, and D. P. Huston. 2003. Biology of common β receptor–signaling cytokines: IL-3, IL-5, and GM-CSF. *J. Allergy Clin. Immunol.* 112: 653–665.

27. Shibata, Y., P.-Y. Berclaz, Z. C. Chroneos, M. Yoshida, J. A. Whitsett, and B. C. Trapnell. 2001. GM-CSF regulates alveolar macrophage differentiation and innate immunity in the lung through PU. 1. *Immunity* 15: 557–567.

28. Yoshida, M., M. Ikegami, J. A. Reed, Z. C. Chroneos, and J. A. Whitsett. 2001. GM-CSF regulates protein and lipid catabolism by alveolar macrophages. *Am. J. Physiol. Lung Cell Mol. Physiol.* 280: L379–L386.

29. Shoji, N., Y. Ito, Y. Kimura, J. Nishimaki, Y. Kuriyama, T. Tauchi, M. Yaguchi, D. Payzulla, Y. Ebihara, and K. Ohyashiki. 2002. Pulmonary alveolar proteinosis as a terminal complication in myelodysplastic syndromes: a report of four cases detected on autopsy. *Leuk. Res.* 26: 591–595.

30. Inoue, Y., B. C. Trapnell, R. Tazawa, T. Arai, T. Takada, N. Hizawa, Y. Kasahara, K. Tatsumi, M. Hojo, T. Ichiwata, N. Tanaka, E. Yamaguchi, R. Eda, K. Oishi, Y. Tsuchihashi, C. Kaneko, T. Nukiwa, M. Sakatani, J. P. Krischer, and K. Nakata. 2008. Characteristics of a Large Cohort of Patients with Autoimmune Pulmonary Alveolar Proteinosis in Japan. *Am J Respir Crit Care Med* 177: 752–762.

31. Ishii, H., R. Tazawa, C. Kaneko, T. Saraya, Y. Inoue, E. Hamano, Y. Kogure, K. Tomii, M. Terada, T. Takada, M. Hojo, A. Nishida, T. Ichiwata, B. C. Trapnell, H. Goto, and K. Nakata. 2011. Clinical features of secondary pulmonary alveolar proteinosis: pre-mortem cases in Japan. *European Respiratory Journal* 37: 465–468.

32. Dirksen, U., U. Hattenhorst, P. Schneider, H. Schroten, U. Göbel, A. Böcking, K.-M. Müller, R. Murray, and S. Burdach. 1998. Defective expression of granulocyte-macrophage colony-stimulating factor/interleukin-3/interleukin-5 receptor common β chain in children with acute myeloid leukemia associated with respiratory failure. *Blood* 92: 1097–1103.

33. Pamuk, G. E., B. Turgut, O. Vural, M. Demir, O. Hatipoğlu, E. Unlü, S. Altaner, M. Gerenli, and B. Cakir. 2003. Pulmonary alveolar proteinosis in a patient with acute lymphoid leukemia regression after G-CSF therapy. *Leuk. Lymphoma* 44: 871–874.

34. Milleron, B. J., U. Costabel, H. Teschler, R. Ziesche, J. L. Cadranel, H. Matthys, and G. M. Akoun. 1991. Bronchoalveolar lavage cell data in alveolar proteinosis. *Am. Rev. Respir. Dis.* 144: 1330–1332.

35. Teschler, H., R. Ziesche, H. Matthys, D. Greschuchna, N. Konietzko, J. Guzman, and U. Costabel. 1990. [Detection of the activation of alveolar lymphocytes in alveolar proteinosis]. *Pneumologie* 44 Suppl 1: 306–307.

36. Szabo, S. J., S. T. Kim, G. L. Costa, X. Zhang, C. G. Fathman, and L. H. Glimcher. 2000. A novel transcription factor, T-bet, directs Th1 lineage commitment. *Cell* 100: 655–669.

37. Lazarevic, V., L. H. Glimcher, and G. M. Lord. 2013. T-bet: a bridge between innate and adaptive immunity. *Nature Reviews Immunology* 13: 777–789.

38. Sullivan, B. M., A. Juedes, S. J. Szabo, M. von Herrath, and L. H. Glimcher. 2003. Antigen-driven effector CD8 T cell function regulated by T-bet. *Proc. Natl. Acad. Sci. U.S.A.* 100: 15818–15823.

39. Joshi, N. S., W. Cui, A. Chandele, H. K. Lee, D. R. Urso, J. Hagman, L. Gapin, and S. M. Kaech. 2007. Inflammation directs memory precursor and short-lived effector CD8(+) T cell fates via the graded expression of T-bet transcription factor. *Immunity* 27: 281–295.

40. Cruz-Guilloty, F., M. E. Pipkin, I. M. Djuretic, D. Levanon, J. Lotem, M. G. Lichtenheld, Y. Groner, and A. Rao. 2009. Runx3 and T-box proteins cooperate to establish the transcriptional program of effector CTLs. *J. Exp. Med.* 206: 51–59.

41. Lazarevic, V., and L. H. Glimcher. 2011. T-bet in disease. *Nature Immunology* 12: 597–606.

42. Neurath, M. F., B. Weigmann, S. Finotto, J. Glickman, E. Nieuwenhuis, H. Iijima, A. Mizoguchi, E. Mizoguchi, J. Mudter, P. R. Galle, A. Bhan, F. Autschbach, B. M. Sullivan, S. J. Szabo, L. H. Glimcher, and R. S. Blumberg. 2002. The transcription factor T-bet regulates mucosal T cell activation in experimental colitis and Crohn's disease. *J. Exp. Med.* 195: 1129–1143.

43. Matsuoka, K., N. Inoue, T. Sato, S. Okamoto, T. Hisamatsu, Y. Kishi, A. Sakuraba, O. Hitotsumatsu, H. Ogata, K. Koganei, T. Fukushima, T. Kanai, M. Watanabe, H. Ishii, and T. Hibi. 2004. T-bet upregulation and subsequent interleukin 12 stimulation are essential for induction of Th1 mediated immunopathology in Crohn's disease. *Gut* 53: 1303–1308.

44. Sasaki, Y., K. Ihara, N. Matsuura, H. Kohno, S. Nagafuchi, R. Kuromaru, K. Kusuhara, R. Takeya, T. Hoey, H. Sumimoto, and T. Hara. 2004. Identification of a novel type 1 diabetes susceptibility gene, T-bet. *Hum. Genet.* 115: 177–184.

45. Sloand, E., S. Kim, J. P. Maciejewski, J. Tisdale, D. Follmann, and N. S. Young. 2002. Intracellular interferon-gamma in circulating and marrow T cells detected by flow cytometry and the response to immunosuppressive therapy in patients with aplastic anemia. *Blood* 100: 1185–1191.

46. Chen, J., K. Lipovsky, F. M. Ellison, R. T. Calado, and N. S. Young. 2004. Bystander destruction of hematopoietic progenitor and stem cells in a mouse model of infusion-induced bone marrow failure. *Blood* 104: 1671–1678.

47. Solomou, E. E., K. Keyvanfar, and N. S. Young. 2006. T-bet, a Th1 transcription factor, is up-regulated in T cells from patients with aplastic anemia. *Blood* 107: 3983–3991.

48. Finotto, S., M. F. Neurath, J. N. Glickman, S. Qin, H. A. Lehr, F. H. Y. Green, K. Ackerman, K. Haley, P. R. Galle, S. J. Szabo, J. M. Drazen, G. T. De Sanctis, and L. H. Glimcher. 2002. Development of spontaneous airway changes consistent with human asthma in mice lacking T-bet. *Science* 295: 336–338.

49. Zhumabekov, T., P. Corbella, M. Tolaini, and D. Kioussis. 1995. Improved version of a human CD2 minigene based vector for T cell-specific expression in transgenic mice. *J. Immunol. Methods* 185: 133–140.

50. Kondo, Y., M. Iizuka, E. Wakamatsu, Z. Yao, M. Tahara, H. Tsuboi, M. Sugihara, T. Hayashi, K. Yoh, S. Takahashi, I. Matsumoto, and T. Sumida. 2011. Overexpression of T-bet gene regulates murine autoimmune arthritis. *Arthritis & Rheumatism* 64: 162–172.

51. Ishizaki, K., A. Yamada, K. Yoh, T. Nakano, H. Shimohata, A. Maeda, Y. Fujioka, N. Morito, Y. Kawachi, K. Shibuya, F. Otsuka, A. Shibuya, and S. Takahashi. 2007. Th1 and type 1 cytotoxic T cells dominate responses in T-bet overexpression transgenic mice that develop contact dermatitis. *J. Immunol.* 178: 605–612.

52. Li, H., and R. Durbin. 2009. Fast and accurate short read alignment with Burrows-Wheeler transform. *Bioinformatics* 25: 1754–1760.

53. Iyonaga, K., M. Suga, T. Yamamoto, H. Ichiyasu, H. Miyakawa, and M. Ando. 1999. Elevated bronchoalveolar concentrations of MCP-1 in patients with pulmonary alveolar proteinosis. *Eur. Respir. J.* 14: 383–389.

54. Nakano, H., J. E. Burgents, K. Nakano, G. S. Whitehead, C. Cheong, C. D. Bortner, and D. N. Cook. 2013. Migratory properties of pulmonary dendritic cells are determined by their developmental lineage. *Mucosal Immunol* 6: 678–691.

55. Schulz, C., E. G. Perdiguero, L. Chorro, H. Szabo-Rogers, N. Cagnard, K. Kierdorf, M. Prinz, B. Wu, S. E. W. Jacobsen, J. W. Pollard, J. Frampton, K. J. Liu, and F. Geissmann. 2012. A Lineage of Myeloid Cells Independent of Myb and Hematopoietic Stem Cells. *Science* 336: 86–90.

56. Yona, S., K.-W. Kim, Y. Wolf, A. Mildner, D. Varol, M. Breker, D. Strauss-Ayali, S. Viukov, M. Guilliams, A. Misharin, D. A. Hume, H. Perlman, B. Malissen, E. Zelzer, and S. Jung. 2013. Fate Mapping Reveals Origins and Dynamics of Monocytes and Tissue Macrophages under Homeostasis. *Immunity* 38: 79–91.

57. Fogg, D. K., C. Sibon, C. Miled, S. Jung, P. Aucouturier, D. R. Littman, A. Cumano, and F. Geissmann. 2006. A clonogenic bone marrow progenitor specific for macrophages and dendritic cells. *Science* 311: 83–87.

58. Jennings, V. M., D. L. Dillehay, S. K. Webb, and L. A. Brown. 1995. Pulmonary alveolar proteinosis in SCID mice. *Am J Respir Cell Mol Biol* 13: 297–306.

59. Nakamura, A., R. Ebina-Shibuya, A. Itoh-Nakadai, A. Muto, H. Shima, D. Saigusa, J. Aoki, M. Ebina, T. Nukiwa, and K. Igarashi. 2013. Transcription repressor Bach2 is required for pulmonary surfactant homeostasis and alveolar macrophage function. *J. Exp. Med.* 139: 14.

60. Dorfman, D. M., E. S. Hwang, A. Shahsafaei, and L. H. Glimcher. 2004. T-bet, a T-cell-associated transcription factor, is expressed in a subset of B-cell lymphoproliferative disorders. *Am. J. Clin. Pathol.* 122: 292–297.

61. Sherman, M. J., C. A. Hanson, and J. D. Hoyer. 2011. An assessment of the usefulness of immunohistochemical stains in the diagnosis of hairy cell leukemia. *Am. J. Clin. Pathol.* 136: 390–399.

62. Shinkai, Y., G. Rathbun, K. P. Lam, E. M. Oltz, V. Stewart, M. Mendelsohn, J. Charron, M. Datta, F. Young, and A. M. Stall. 1992. RAG-2-deficient mice lack mature lymphocytes owing to inability to initiate V(D)J rearrangement. *Cell* 68: 855–867.

63. Singbartl, K., J. Thatte, M. L. Smith, K. Wethmar, K. Day, and K. Ley. 2001. A CD2-green fluorescence protein-transgenic mouse reveals very late antigen-4-dependent CD8+ lymphocyte rolling in inflamed venules. *J. Immunol.* 166: 7520–7526.

64. Townsend, M. J., A. S. Weinmann, J. L. Matsuda, R. Salomon, P. J. Farnham, C. A. Biron, L. Gapin, and L. H. Glimcher. 2004. T-bet regulates the terminal maturation and homeostasis of NK and Valpha14i NKT cells. *Immunity* 20: 477–494.

65. Matsuda, J. L. 2006. T-bet concomitantly controls migration, survival, and effector functions during the development of V 14i NKT cells. *Blood* 107: 2797–2805.

66. Sieweke, M. H., and J. E. Allen. 2013. Beyond Stem Cells: Self-Renewal of Differentiated Macrophages. *Science* 342: 1242974–1242974.

67. Jenkins, S. J., D. Ruckerl, P. C. Cook, L. H. Jones, F. D. Finkelman, N. van Rooijen, A. S. MacDonald, and J. E. Allen. 2011. Local Macrophage Proliferation, Rather than Recruitment from the Blood, Is a Signature of TH2 Inflammation. *Science* 332: 1284–1288.

68. Ginhoux, F., M. Greter, M. Leboeuf, S. Nandi, P. See, S. Gokhan, M. F. Mehler, S. J. Conway, L. G. Ng, E. R. Stanley, I. M. Samokhvalov, and M. Merad. 2010. Fate mapping analysis reveals that adult microglia derive from primitive macrophages. *Science* 330: 841–845.

69. Ajami, B., J. L. Bennett, C. Krieger, W. Tetzlaff, and F. M. V. Rossi. 2007. Local self-renewal can sustain CNS microglia maintenance and function throughout adult life. *Nat. Neurosci.* 10: 1538–1543.

70. Wynn, T. A., A. Chawla, and J. W. Pollard. 2013. Macrophage biology in development, homeostasis and disease. *Nature* 496: 445–455.

71. Guilliams, M., I. De Kleer, S. Henri, S. Post, L. Vanhoutte, S. De Prijck, K. Deswarte, B. Malissen, H. Hammad, and B. N. Lambrecht. 2013. Alveolar macrophages develop from fetal monocytes that differentiate into long-lived cells in the first week of life via GM-CSF. *J. Exp. Med.*

72. Broug-Holub, E., G. B. Toews, J. F. van Iwaarden, R. M. Strieter, S. L. Kunkel, R. Paine, and T. J. Standiford. 1997. Alveolar macrophages are required for protective pulmonary defenses in murine Klebsiella pneumonia: elimination of alveolar macrophages increases neutrophil recruitment but decreases bacterial clearance and survival. *Infection and Immunity* 65: 1139–1146.

73. Ghoneim, H. E., P. G. Thomas, and J. A. McCullers. 2013. Depletion of Alveolar Macrophages during Influenza Infection Facilitates Bacterial Superinfections. *J. Immunol.*

74. Maus, U., J. Huwe, R. Maus, W. Seeger, and J. Lohmeyer. 2001. Alveolar JE/MCP-1 and endotoxin synergize to provoke lung cytokine upregulation, sequential neutrophil and monocyte influx, and vascular leakage in mice. *Am J Respir Crit Care Med* 164: 406–411.

75. Landsman, L., C. Varol, and S. Jung. 2007. Distinct differentiation potential of blood monocyte subsets in the lung. *J. Immunol.* 178: 2000–2007.

76. Gordon, S., and P. R. Taylor. 2005. Monocyte and macrophage heterogeneity. *Nature Reviews Immunology* 5: 953–964.

77. Hashimoto, D., A. Chow, C. Noizat, P. Teo, M. B. Beasley, M. Leboeuf, C. D. Becker, P. See, J. Price, D. Lucas, M. Greter, A. Mortha, S. W. Boyer, E. C. Forsberg, M. Tanaka, N. van Rooijen, A. García-Sastre, E. R. Stanley, F. Ginhoux, P. S. Frenette, and M. Merad. 2013. Tissue-Resident Macrophages Self-Maintain Locally throughout Adult Life with Minimal Contribution from Circulating Monocytes. *Immunity* 38: 792–804.

78. Gautier, E. L., A. Chow, R. Spanbroek, G. Marcelin, M. Greter, C. Jakubzick, M. Bogunovic, M. Leboeuf, N. van Rooijen, A. J. Habenicht, M. Merad, and G. J. Randolph. 2012. Systemic analysis of PPARγ in mouse macrophage populations reveals marked diversity in expression with critical roles in resolution of inflammation and airway immunity. *J. Immunol.* 189: 2614–2624.

79. Boring, L., J. Gosling, S. W. Chensue, S. L. Kunkel, R. V. Farese, H. E. Broxmeyer, and I. F. Charo. 1997. Impaired monocyte migration and reduced type 1 (Th1) cytokine responses in C-C chemokine receptor 2 knockout mice. *J. Clin. Invest.* 100: 2552–2561.

80. Mack, M., J. Cihak, C. Simonis, B. Luckow, A. E. Proudfoot, J. Plachý, H. Brühl, M. Frink, H. J. Anders, V. Vielhauer, J. Pfirstinger, M. Stangassinger, and D. Schlöndorff. 2001. Expression and characterization of the chemokine receptors CCR2 and CCR5 in mice. *J. Immunol.* 166: 4697–4704.

81. Takizawa, H., S. Boettcher, and M. G. Manz. 2012. Demand-adapted regulation of early hematopoiesis in infection and inflammation. *Blood* 119: 2991–3002.

82. Griseri, T., B. S. McKenzie, C. Schiering, and F. Powrie. 2012. Dysregulated hematopoietic stem and progenitor cell activity promotes interleukin-23-driven chronic intestinal inflammation. *Immunity* 37: 1116–1129.

83. Tsuda, H., and H. Yamasaki. 2000. Type I and type II T-cell profiles in aplastic anemia and refractory anemia. *Am. J. Hematol.* 64: 271–274.

84. Hamdi, W., H. Ogawara, H. Handa, N. Tsukamoto, and H. Murakami. 2009. Clinical significance of Th1/Th2 ratio in patients with myelodysplastic syndrome. *International Journal of Laboratory Hematology* 31: 630–638.

85. Jacobs, N. L., S. G. Holtan, L. F. Porrata, S. N. Markovic, A. Tefferi, and D. P. Steensma. 2010. Host immunity affects survival in myelodysplastic syndromes: Independent prognostic value of the absolute lymphocyte count. *Am. J. Hematol.* 85: 160–163.

86. Sloand, E. M., J. J. Melenhorst, Z. C. G. Tucker, L. Pfannes, J. M. Brenchley, A. Yong, V. Visconte, C. Wu, E. Gostick, P. Scheinberg, M. J. Olnes, D. C. Douek, D. A. Price, A. J. Barrett, and N. S. Young. 2011. T-cell immune responses to Wilms tumor 1 protein in myelodysplasia responsive to immunosuppressive therapy. *Blood* 117: 2691–2699.

87. Young, N. S. 1996. Immune pathophysiology of acquired aplastic anaemia. *European Journal of Haematology* 57: 55–59.

88. Nakao, S., X. Feng, and C. Sugimori. 2005. Immune Pathophysiology of Aplastic Anemia. *Int J Hematol* 82: 196–200.

89. Malur, A., A. J. Mccoy, S. Arce, B. P. Barna, M. S. Kavuru, A. G. Malur, and M. J. Thomassen. 2009. Deletion of PPARγ in alveolar macrophages is associated with a Th-1 pulmonary inflammatory response. *J. Immunol.* 182: 5816–5822.

Figures and Tables

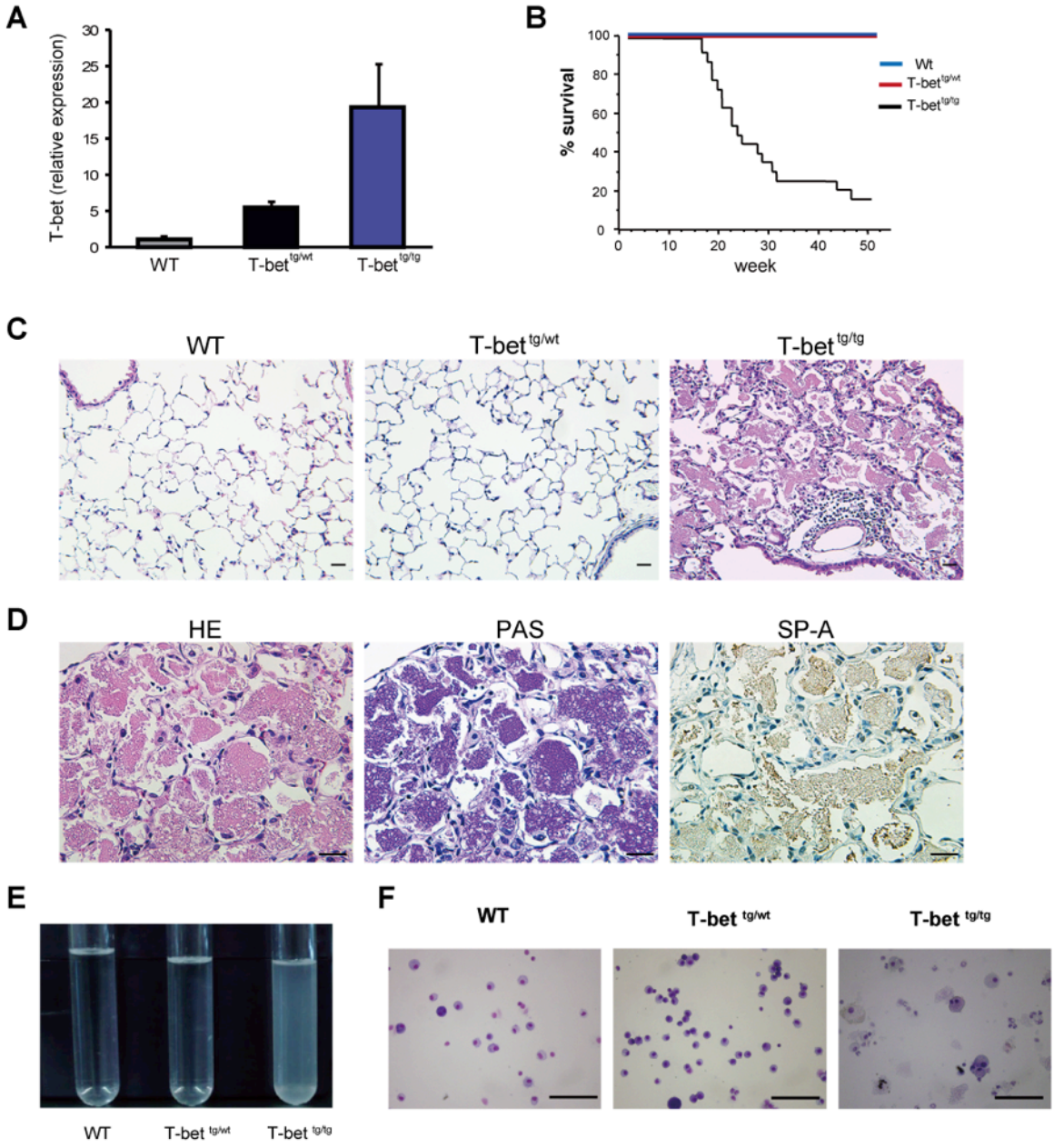

Figure 1

Aged T-bet$^{tg/tg}$ mice spontaneously develop PAP-like disease.

(**A**) T-bet mRNA expression levels in the lungs of WT, T-bet$^{tg/wt}$, and T-bet$^{tg/tg}$ mice at 50 wk of age. (**B**) Survival monitoring results of mice with the indicated genotypes. n=20 in each group. (**C**) Representative microphotographs of the lungs of WT, T-bet$^{tg/wt}$, and T-bet$^{tg/tg}$ mice at 50 wk of age. Alveolar spaces of T-bet$^{tg/tg}$ mice are filled with acellular eosinophilic materials with inflammatory cell infiltration. Hematoxylin and eosin (HE) staining. Bar = 100μm. (**D**) Microphotographs of the lung of T-bet$^{tg/tg}$ mice. The alveolar materials are positive for PAS staining and immunohistochemical staining of mouse SP-A. Bar = 100μm. (**E**) Appearance of BAL fluids of WT, T-bet$^{tg/wt}$, and T-bet$^{tg/tg}$ mice at 50 wk of age. (**F**) Cytology of BAL cells obtained from WT, T-bet$^{tg/wt}$, and T-bet$^{tg/tg}$ mice at 50 wk of age stained with hemacolor (Bar = 100 μm).

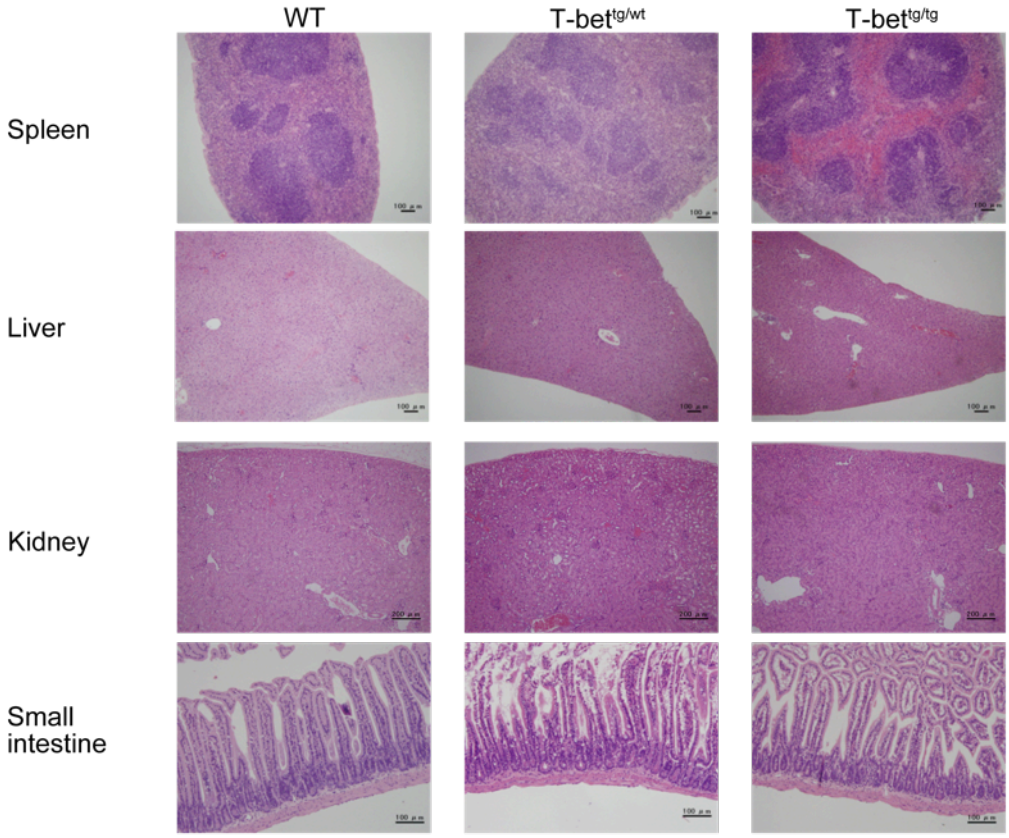

Figure 2

Histopathological analyses of hCD2-T-bet tg mice

H&E stainings of the spleen, liver, kidney, and small intestine sections of WT, T-bet$^{tg/wt}$, and T-bet$^{tg/tg}$ mice at 50 weeks of age. Bar = 100 μm.

A

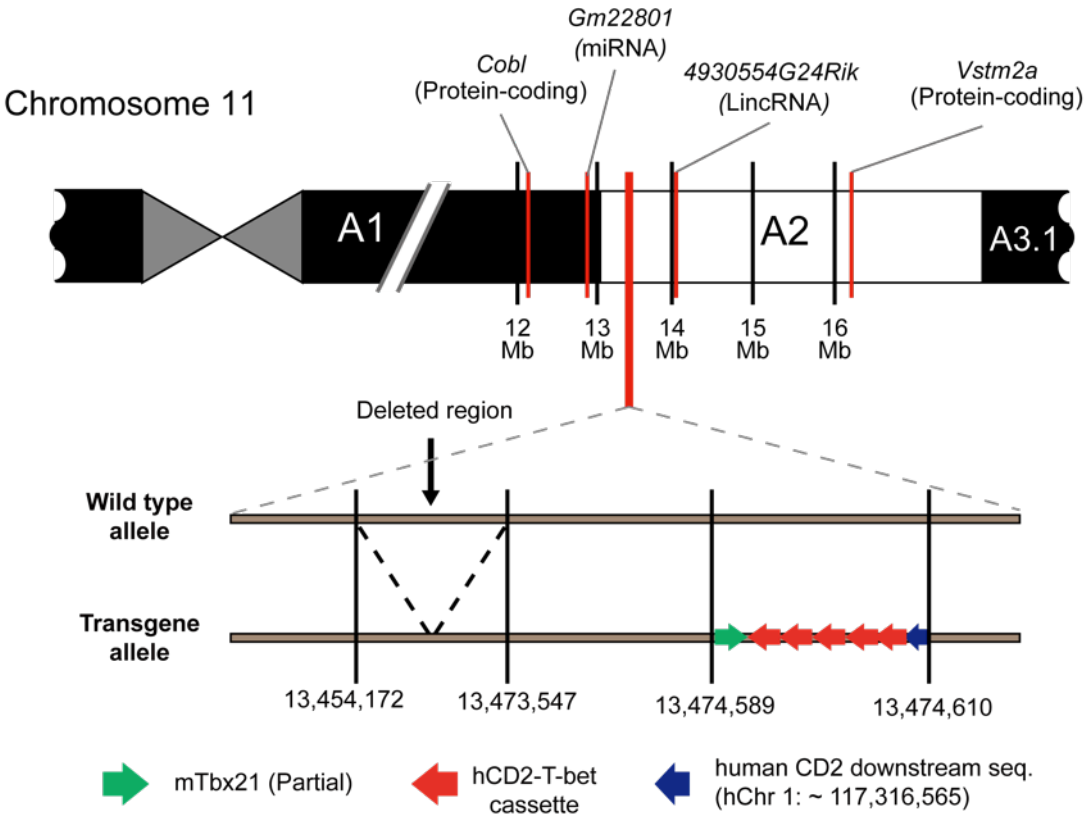

Figure 3

Identification of the transgene integration locus.

(**A**) A schamatic of the region around the transgene integration site and its neighboring genes, including protein-codings and non-coding RNAs in the chromosome 11. Cobl: cordon-blue WH2 repeat; Vstm2a: v-set and transmembrane domain containing 2A; miRNA: microRNA; LincRNA: Large intergenic non-coding RNA.

(Legend continued on next page)

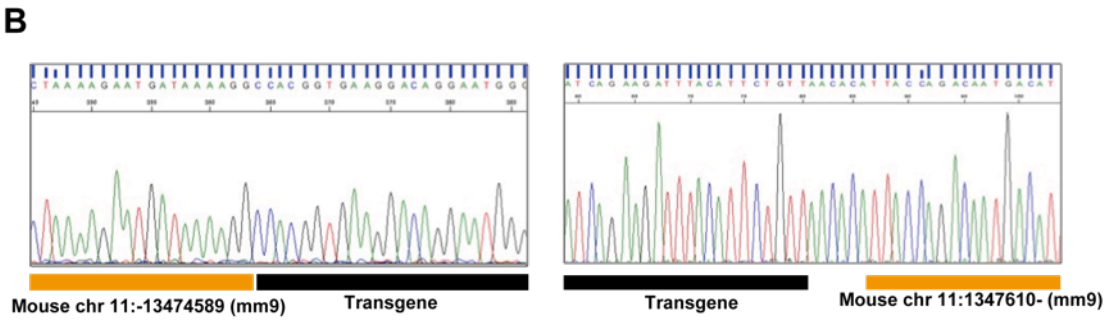

Figure Legend (Continued)

(**B**) The results of direct sequencings around the potential transgene integration region using the primers indicated in Table 1. (**C**) A representative electrophoresis image of PCR products amplified with the designated primer pairs from genomic DNA extracted from the tail tips of mice with indicated genotypes.

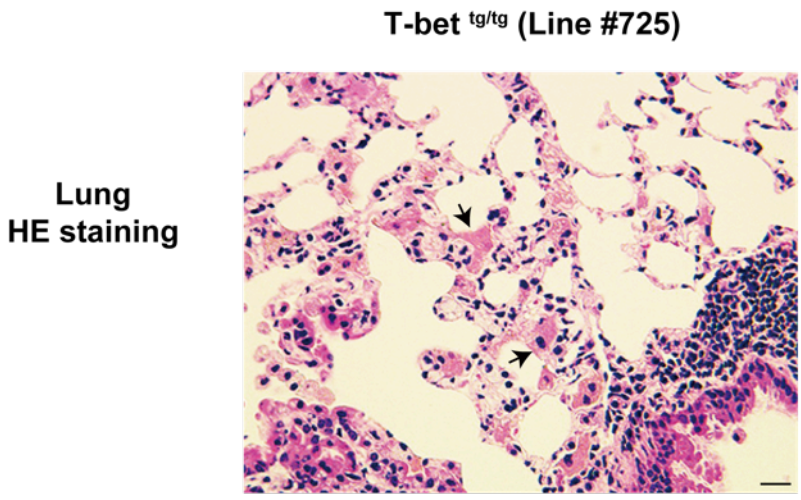

Figure 4

Lung section of T-bet$^{tg/tg}$ mice from other line.

A representative image of HE staining of lung tissue section obtained from a T-bet$^{tg/tg}$ mouse of other transgenic line (#725) at 50 weeks of age. The arrowheads indicate accumulation of eosinophilic materials as observed in T-bet$^{tg/tg}$ lungs of the current line (#731). Interstitial infiltration of lymphocytes are observed (lower right). Scale bar = 100 μm.

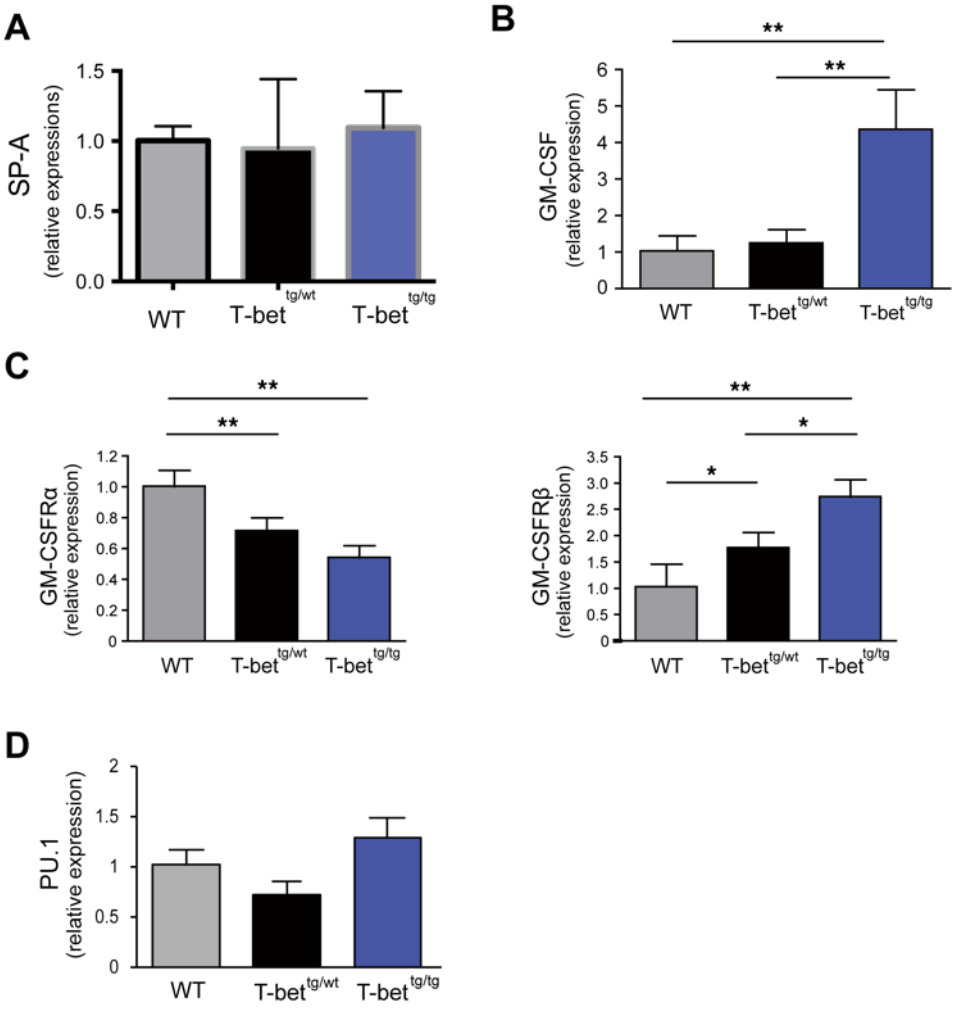

Figure 5

Gene expression analysis for GM-CSF signaling in the lung of T-bet tg mice

(**A**) Expression of SP-A mRNA in the lungs of WT, T-bet$^{tg/wt}$, and T-bet$^{tg/tg}$ mice at 50 wk of age. (**B**) Expression of GM-CSF mRNA in the lungs of WT, T-bet$^{tg/wt}$, and T-bet$^{tg/tg}$ mice at 50 wk of age. (**C** and **D**) Expression of alpha- and beta-chains of the GM-CSF receptor (**C**) and PU.1 (**D**) in macrophages obtained from WT, T-bet$^{tg/wt}$, and T-bet$^{tg/tg}$ mice at 50 wk of age. Mean ± SD; n = 4; *, $P < 0.05$, **, $P < 0.01$ (one-way ANOVA followed by Tukey's multiple comparisons tests).

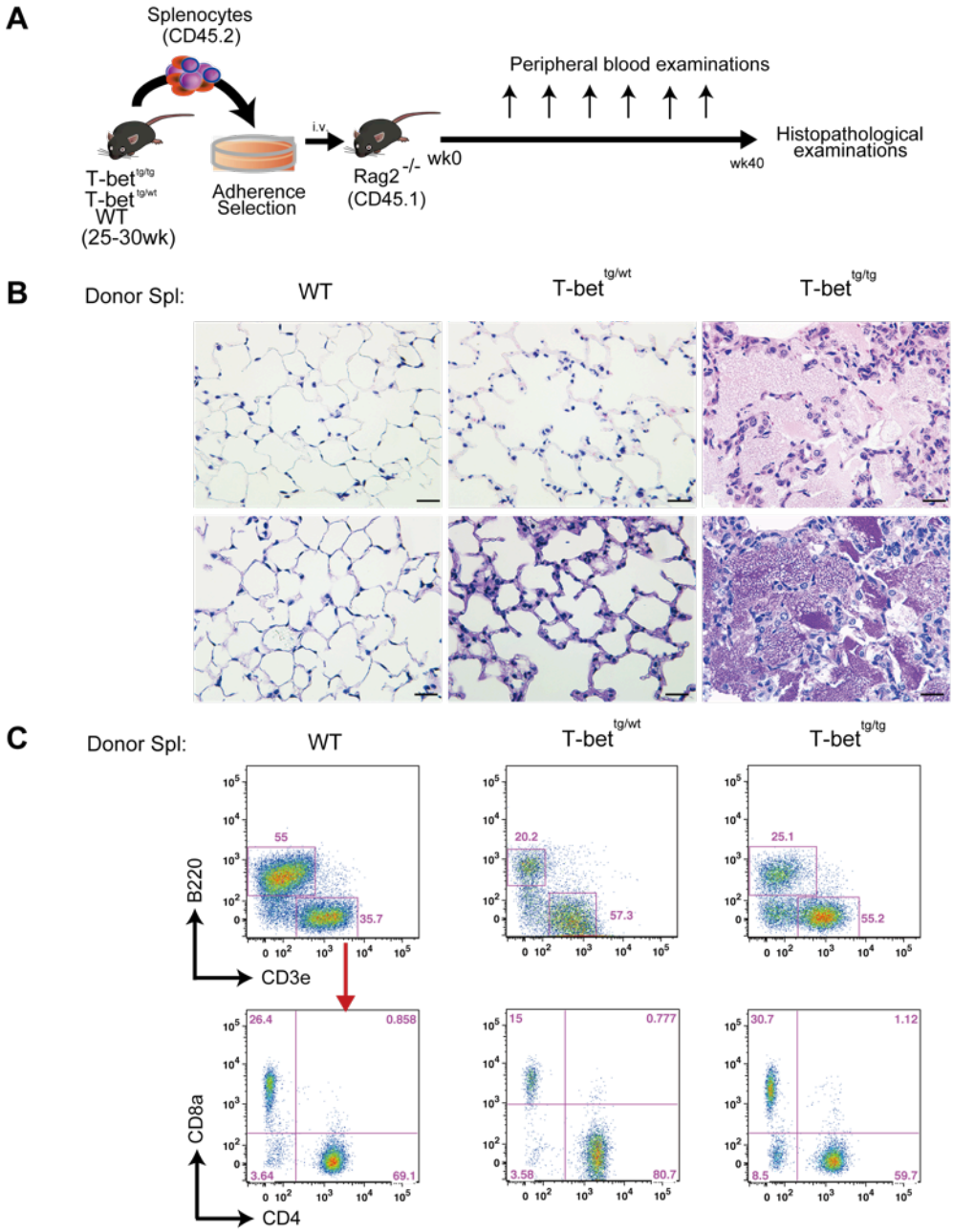

Figure 6

Overexpression of T-bet in lymphocytes initiates PAP development.

(**A**) Diagram of experimental design. (**B**) Representative microphotographs of the lungs of Rag2$^{-/-}$ recipients transplanted with splenocytes from WT, T-bet$^{tg/wt}$, and T-bet$^{tg/tg}$ mice. HE (upper panels) and PAS (lower panels) stainings. Bar = 100μm. (**C**) Representative flow cytometry diagrams showing donor-derived lymphocyte subpopulations in the spleens of recipients that received splenocytes from the indicated genotypes.

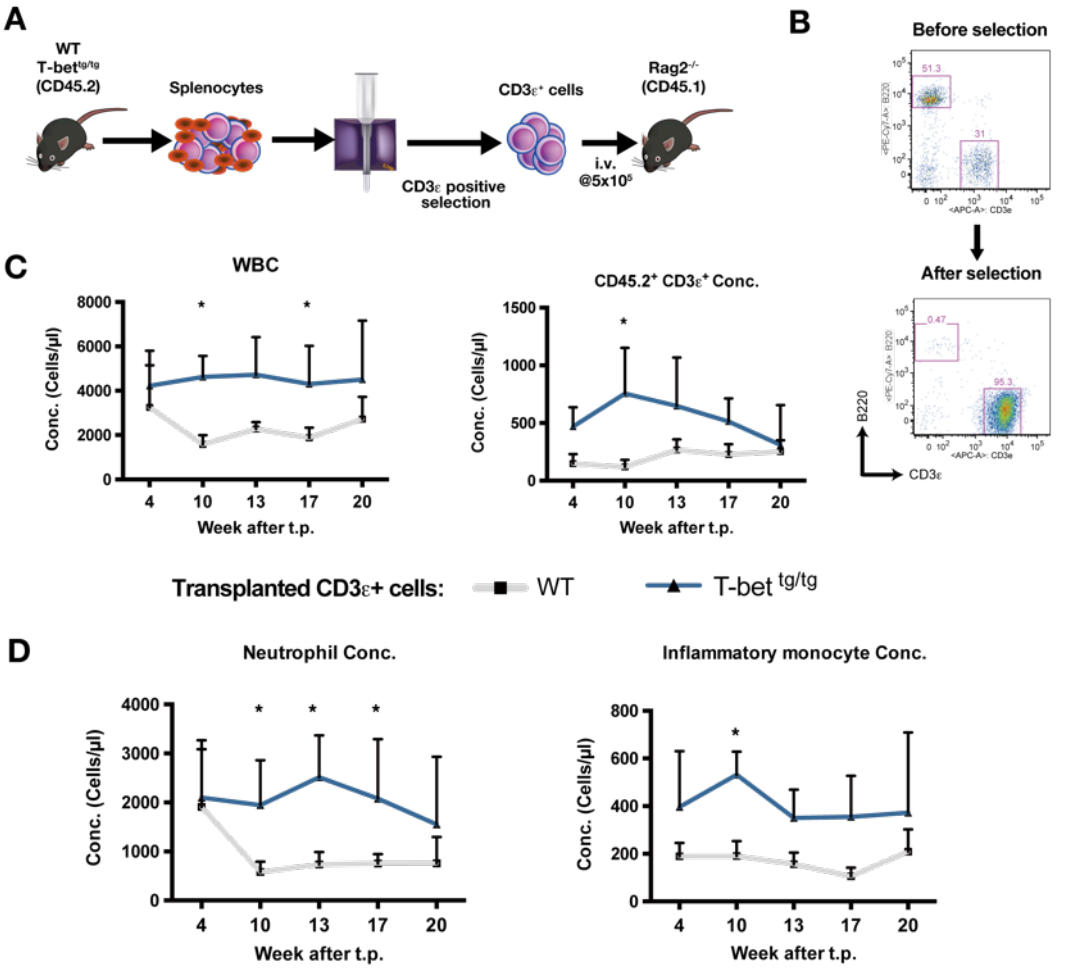

Figure 7

Adoptive transfer of CD3ε⁺ T cells into *Rag2*$^{-/-}$ recipients.

(**A**) The experimental protocol. (**B**) A flow diagram showing the expressions of B220 and CD3ε of splenocytes obtained from a WT spleen before (Left) and after (Right) CD3ε positive selection. (**C**) Transitions of WBC (Left) and donor CD3ε^{+} T cell frequencies (Right) in PB obtained from *Rag2*$^{-/-}$ recipients received WT (Blue line) and T-bet$^{tg/tg}$ (Green line) mice at the indicated week after transplantation (t.p.). Results are expressed as mean ± SD (n = 4 each). (**D**) Transitions of recipient-derived (CD45.1^{+}) inflammatory monocytes frequencies (Left) and neutrophil frequencies (Right) in PB obtained from *Rag2*$^{-/-}$ recipients received WT (Blue line) and T-bet$^{tg/tg}$ (Green line) mice at the indicated week after transplantation (t.p.). Results are expressed as mean ± SD (n = 4 each). The p-values were determined by two-tailed Student' s t tests. *, $P < 0.05$; **, $P < 0.01$.

(Legend continued on next page)

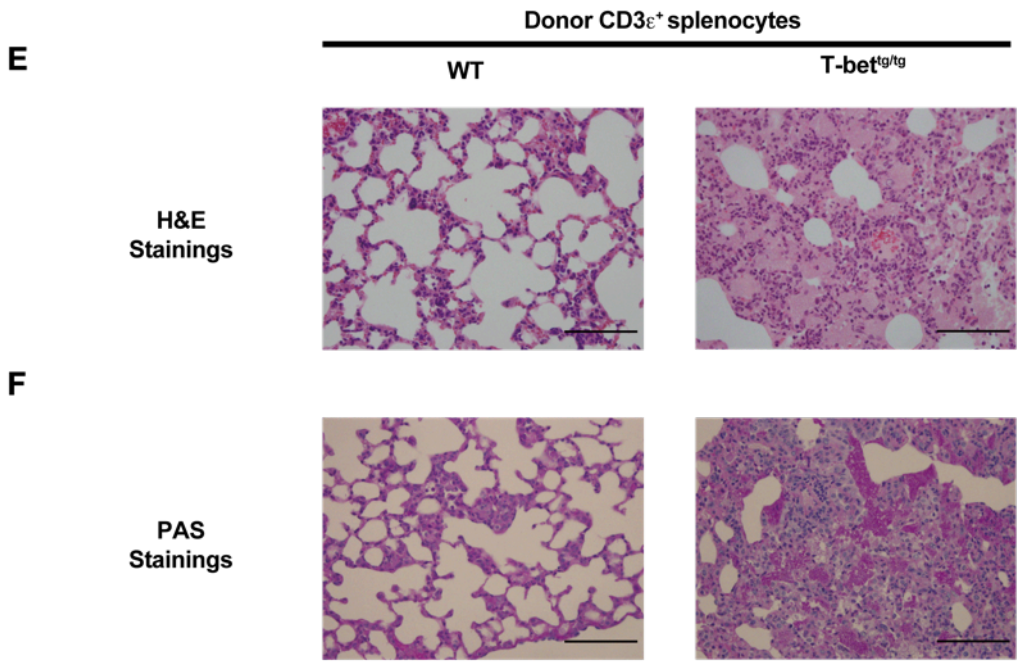

Figure Legend (continued)

(**E**) H&E stainings of lung sections from *Rag2*$^{-/-}$ recipients transplanted with WT (Left) and T-bet$^{tg/tg}$ (Right) T cells. Scale bar = 100 μm. (**F**) PAS stainings of lung sections from *Rag2*$^{-/-}$ recipients transplanted with WT (Left) and T-bet$^{tg/tg}$ (Right) T cells. Scale bar = 100 μm.

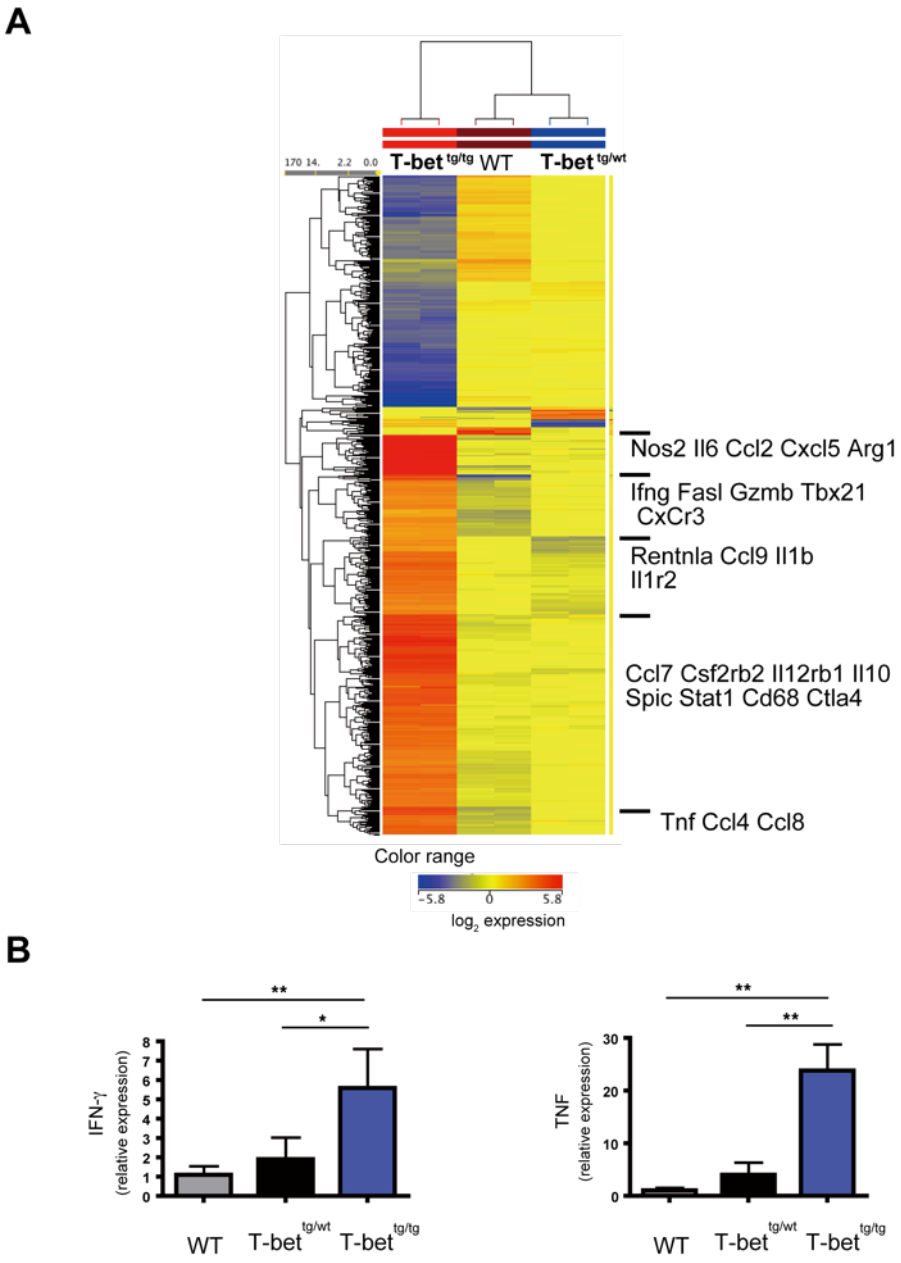

Figure 8

Microarray analysis of lung mRNAs from T-bet tg mice

(**A**) The heat-map of genes whose expression changes are > 10-fold between the genotypes in lung mRNAs. Representatives of genes showed higher expressions in T-bet$^{tg/tg}$ lung mRNAs are listed. (**B**) Levels of IFN-g, and TNF mRNA expressions in lungs from 50-wk-old WT, T-bet$^{tg/wt}$, and T-bet$^{tg/tg}$ mice. n = 4 in each group. Mean ± SD; n = 4; *, $p < 0.05$, **, $p < 0.01$ (one-way ANOVA followed by Tukey' s multiple comparisons tests).

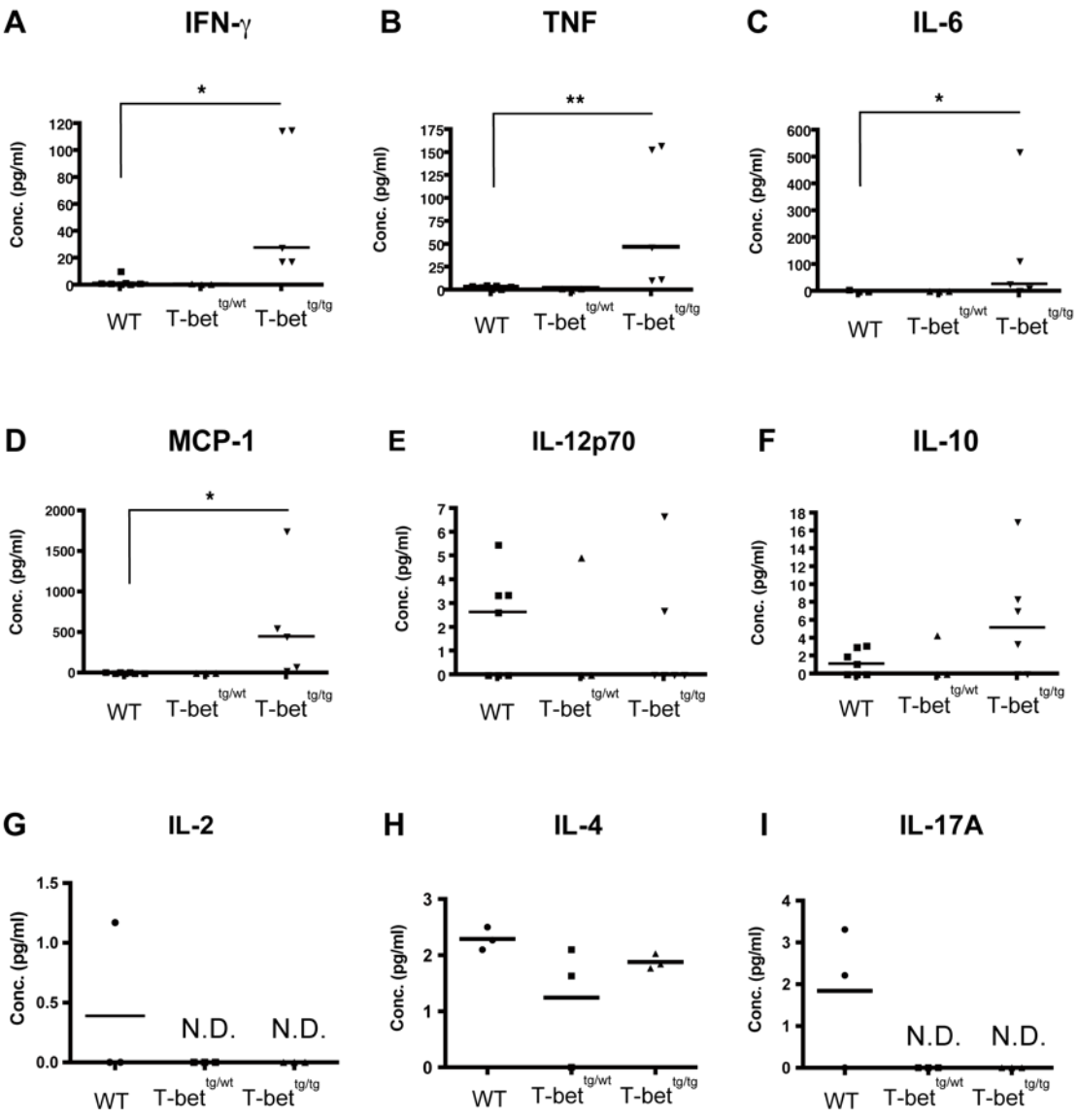

Figure 9

Proinflammatory cytokine productions are enhanced in the lungs of PAP mice.

(**A-F**) Concentrations of IFN-γ (**A**), TNF (**B**), IL-6 (**C**), MCP-1 (**D**), IL-12p70 (**E**), IL-10 (**F**), IL-2 (**G**), IL-4 (**H**), and IL-17A (**I**) in the BAL fluids of WT, T-bet$^{tg/wt}$, and T-bet$^{tg/tg}$ mice at 30-50 wk of age. n = 7, 3 and 5 (A-F). n = 3 (G-I); **, $P < 0.01$; *, $P < 0.05$ (Kruskal Wallis H test followed by Dunn's multiple comparisons test).

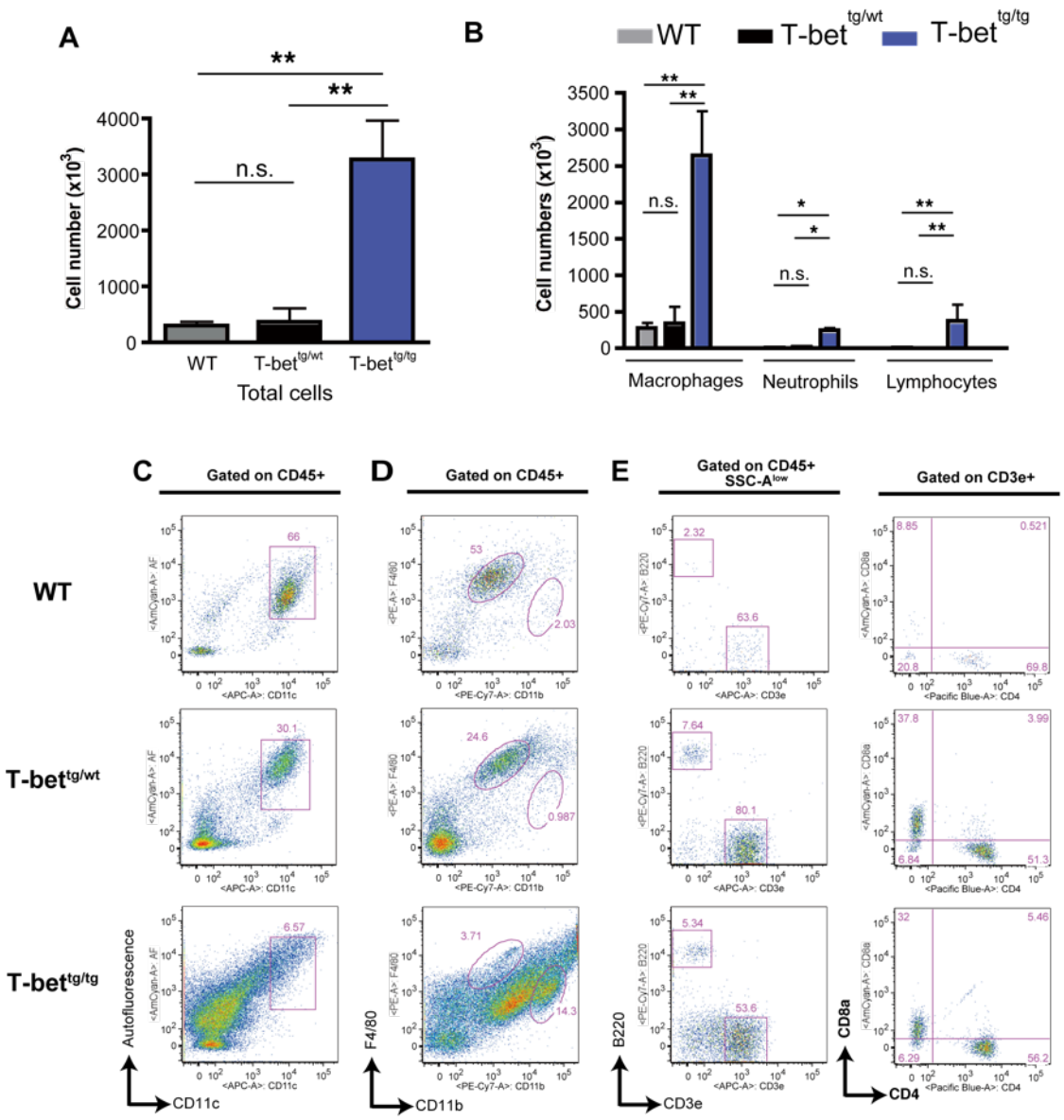

Figure 10
Phenotypic and functional analysis of BAL cells

(**A** and **B**) The number of BAL cells (**A**), macrophages, neutrophils, and lymphocytes (**B**) of BAL fluids of mice WT, T-bet$^{tg/wt}$, and T-bet$^{tg/tg}$ mice at 50 wk of age. Mean ± SD; n = 3. **, $p < 0.01$; *, $p < 0.05$ (one-way ANOVA followed by Tukey's multiple comparisons tests). (**C-E**) Flow cytometry profiles showing the alveolar macrophages (**C**), BM-derived macrophages (**D**) and lymphocytes (**E**) in BAL-recovered cells gated on the leukocyte population (CD45+ cells). Data are a representative of at least three mice.

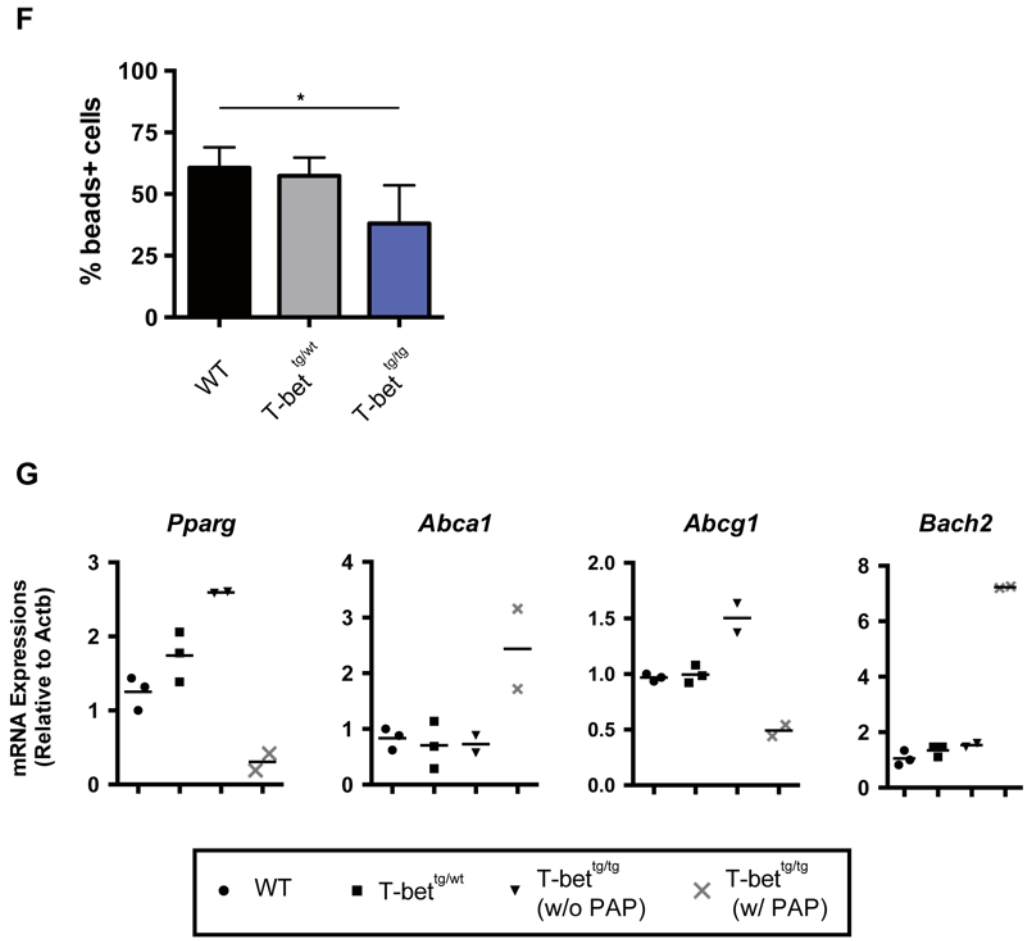

Figure Legend (continued)

(**F**) Frequencies of FITC-beads-positive macrophages obtained from WT, T-bet$^{tg/wt}$, and T-bet$^{tg/tg}$ BAL cells at 50 wk of age. Mean ± SD; n = 4 each; *, $P < 0.05$ (one-way ANOVA followed by Tukey' s multiple comparisons tests). (**G**) Pparg, Abca1, Abcg1, and Bach2 mRNA expression levels in AF+ BAL cells obtained from 35 wks of age. n = 3, 3, 4.

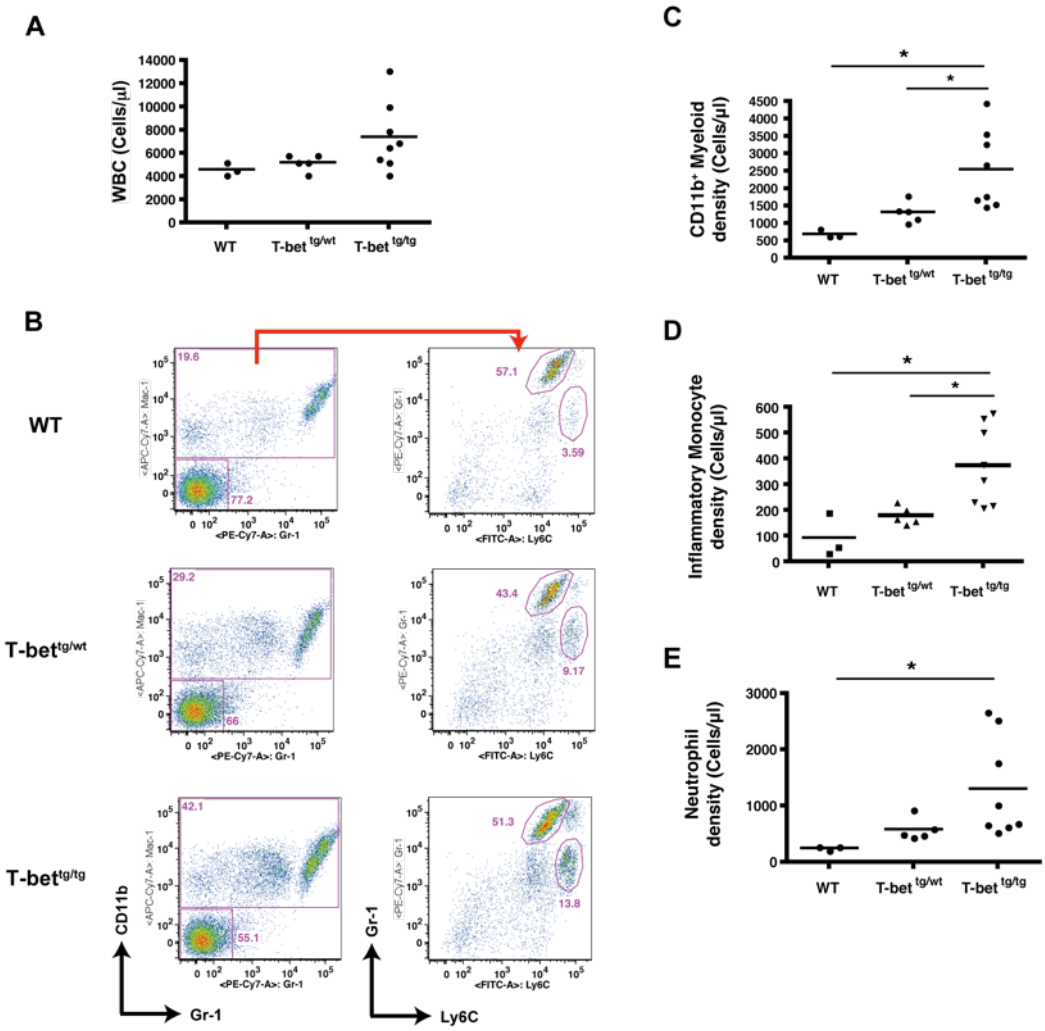

Figure 11

The number of inflammatory monocytes increases in the circulation of PAP mice.

(**A**) White blood cell counts in the peripheral blood of WT, T-bet$^{tg/wt}$, and T-bet$^{tg/tg}$ mice at 25-30 wk of age. (**B**) Representative flow cytometry profiles of the living cell-gated populations (Pi-) in the peripheral blood of each mouse genotype. Myeloid cells were immunophenotypically defined as CD11b^{+}. The myeloid-gated cells were further analyzed for their expression levels of Ly6C and Gr-1. Inflammatory monocytes and neutrophils are defined as Gr-1^{Mid}, Ly6C^{Hi} and Gr-1^{Hi}, Ly6C^{Mid}, respectively. (**C-E**) Numbers of myeloid cells (**C**), inflammatory monocytes (**D**), and neutrophils (**E**) in the peripheral blood from each genotype of mice; *, $p < 0.05$ (one-way ANOVA followed by Tukey' s multiple comparisons tests).

(Legend continued on next page)

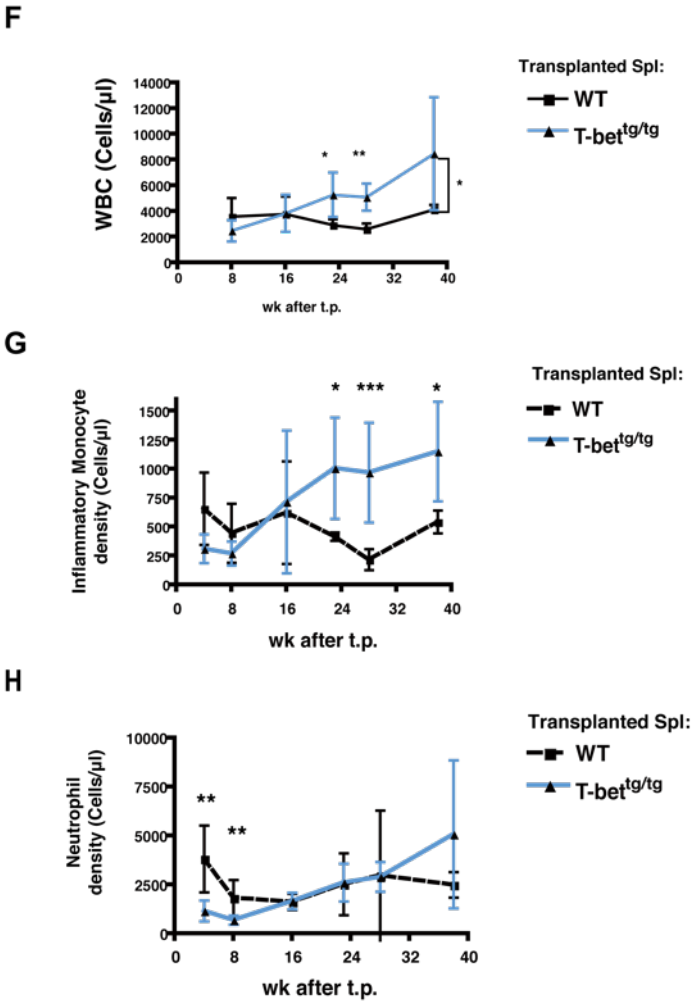

Figure Legend (continued)

(**F**) Changes in white blood cell counts in the peripheral blood of Rag2$^{-/-}$ recipients after transplantation of WT or T-bet$^{tg/tg}$ splenocytes. (**G** and **H**) Changes in the number of inflammatory monocytes (**G**) and neutrophils (**H**) in the peripheral blood of Rag2$^{-/-}$ recipients after transplantation of WT or T-bet$^{tg/tg}$ splenocytes. Mean ± SD; n = 4 and 8; **, $P < 0.01$; *, $P < 0.05$ (Student' s t test).

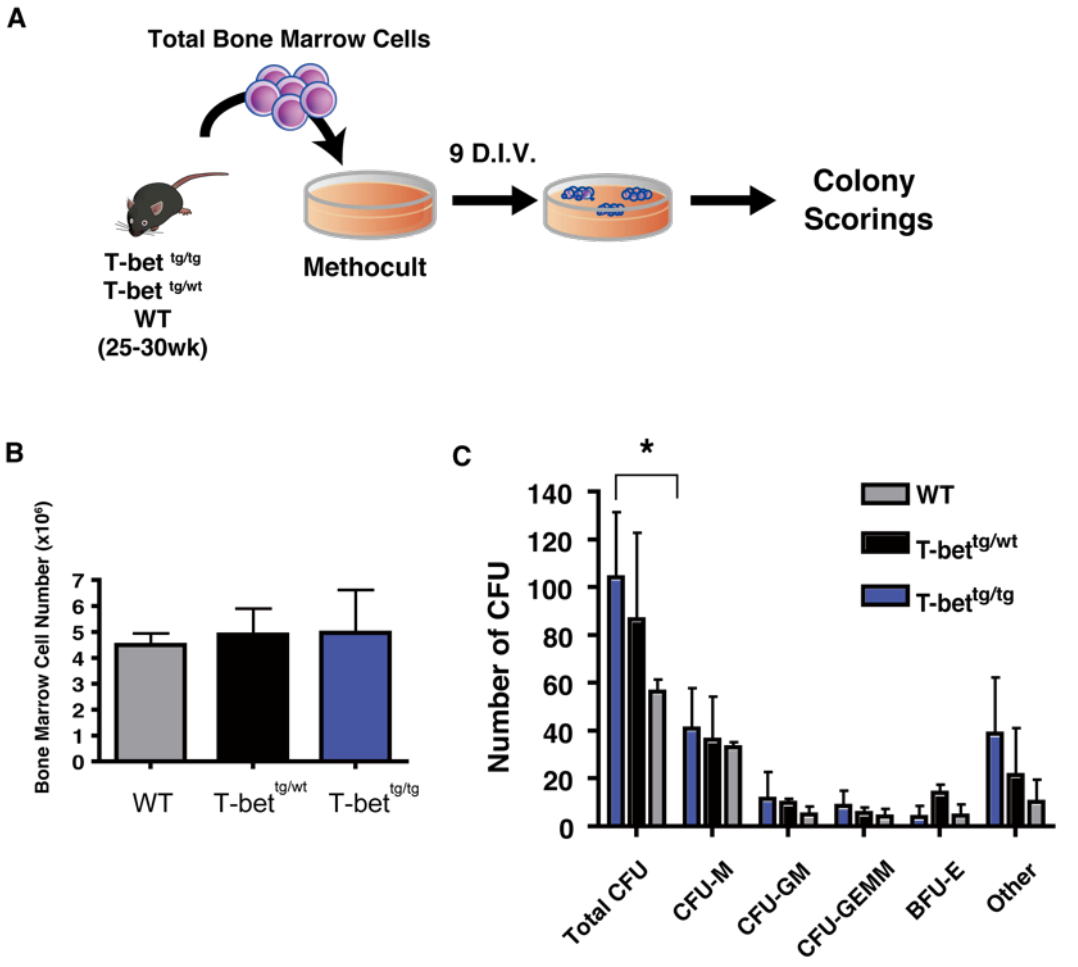

Figure 12

The BM HSPCs from T-bet$^{tg/tg}$ mice acquire monocytic differentiation impairment.

(**A**) The experimental protocol of CFC assays. (**B**) The number of mononuclear cells in a femur of transgenic mice with the indicated genotype. Mean ± SD; n = 3, 3, and 6 (one-way ANOVA followed by Tukey's multiple comparisons tests). (**C**) Results of colony scoring: CFU, colony-forming unit; BFU, blast forming unit; G, granulocyte; E, erythroid; M, macrophage; M, Megakaryocyte. Mean ± SD; n = 5, 4, and 9; *, $P < 0.05$, **, $P < 0.01$ (one-way ANOVA followed by Tukey's multiple comparisons tests).

(Lengend continued on next page)

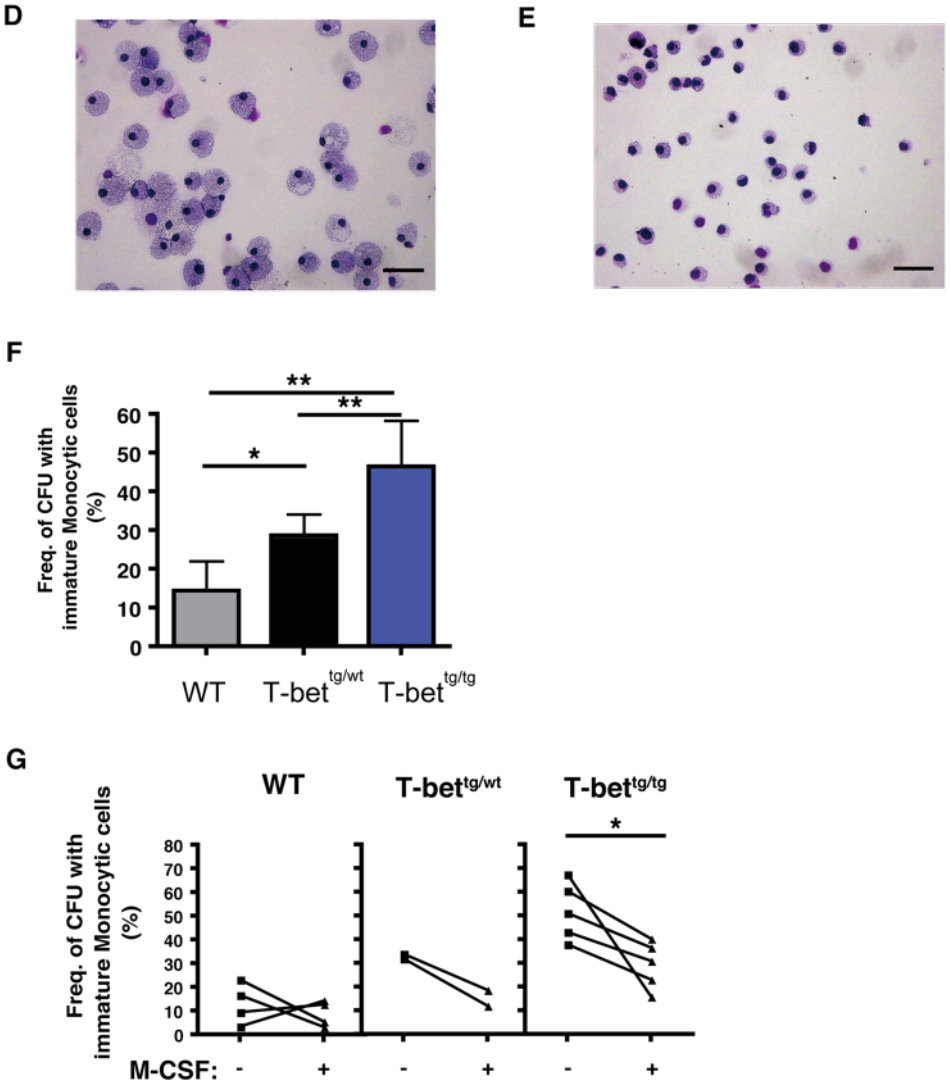

Figure Legend (Continued)

(**D**-**E**) Representative cytospin images showing a terminally matured macrophage colony from the culture with wild-type WBMCs (**D**) and an immature monocytic colony from T-bet$^{tg/tg}$ WBMCs (**E**). Hema-color staining. Bar=50μm. (**F**) Frequencies of colonies containing immature monocytic cells. Mean ± SD; n = 5, 4, and 9; *, $P < 0.05$, **, $P < 0.01$ (two-way ANOVA followed by the SNK tests). (**G**) Effects of M-CSF additions on the frequencies of colonies containing immature monocytic cells. *, $P < 0.05$ (Paired Student' s t test).

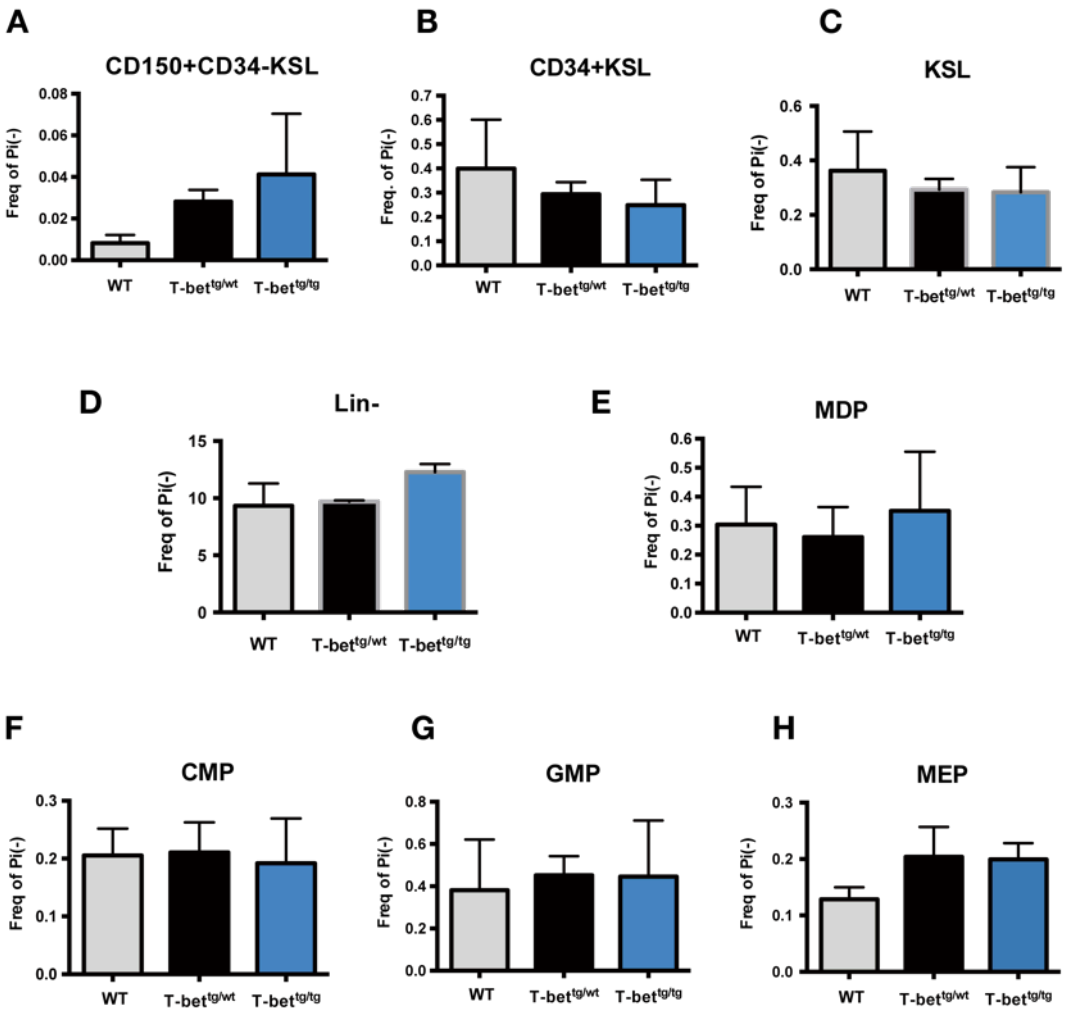

Figure 13

Flowcytometric analysis of BM hematopoietic stem and progenitor cells

Frequencies of hematopoietic stem and progenitor cells in the BM of T-bet tg mice at 30-50 week of ages in the living cells (Pi(-)). (**A**) long-term HSCs (LT-HSC; $CD150^{+}CD34^{-}KSL$), (**B**) $CD34^{+}KSL$, (**C**) KSL, (**D**) Lineage cell $markers^{-}$ (Lin^{-}), (**E**) Monocyte-dendritic cell progenitors (MDP; $Lineage^{-}$ c-kit+ $Sca\text{-}1^{-}$ $CD115^{+}$, CD34+), (**F**) Common myeloid progenitors (CMP; $Lineage^{-}$ c-kit+ $Sca\text{-}1^{-}$ $CD16/32^{-}$ $CD34^{+}$), (**G**) Granulocyte/macrophage progenitors (GMP; $Lineage^{-}$ c-kit+ $Sca\text{-}1^{-}$ $CD16/32^{+}$ $CD34^{+}$), and (**H**) Megakaryocyte/erythrocyte progenitors (MEP; $Lineage^{-}$ c-kit+ $Sca\text{-}1^{-}$ $CD16/32^{-}$ $CD34^{-}$). Results are expressed as mean ± SD (n = 4 each).

	Forward primer	Reverse primer	details
chr11L	CAGCCCAATTTGCTGAGATT	CATTTTGTGGGCATGACATT	5' upstream of the transgene
chr11R	AATCCTTGCCCCAGTGAAAT	TGCATTCTGCTATTGGCTTG	3' downstream of the transgene
genotyping	TGAAGCAAAACCTGCTGCTA	TGTTCTGCACAGTGAAAAGTCA	genotyping primers

Table 1

Sequences of the primers used for transgene integration site determination and genotyping

Chr11F sequence	CTTAGATTTTCAATATGCAAAACATGGATGCCAGAAAATT GTACCTTTAAAAAATATTTAAACTATCTGGTACTAAATGCA TTAAGAAGAACAGAATTGAAGCAAAACCTGCTGCTACTT TTCAAACTTATGAAAGTTTTTAAACCAGGCACAAATGGTT CATGAGGAAACAAGGGAAAATTCTGATCTTTTTAATTGC CACAATTTCTCCCATAGAAAGGAGAACATACCTTCAGGA GGGTTCTTTTTCCATAGGGAAATGTTGGTTATAAGTTCAC CTCTTACTGACTTTTCACTGTGCAGAACATTAAAGGAAC ATATTTATCTATGAATAGAACAATTGGCTAAAAGAATGATA AAAGGCCACGGTGAAGGACAGGAATGGGAACATTCGC CGTCCTTGCTTAGTGATGATCATCTCTGTCTGGTGCTGG TTGAACTTGGACCACAACAGGTGGTTGCTGAGCGCGA CTCTCAGCTTCCCAGACACCTCCAACCCCGCGGGCAA TGCGTAGTCCTCGCGCGGCCCTGGGTAGAGCCCCGC GCGCGGGTCAGGGGCAGGGTAGCCATCCACGGGCGG GTAGCCCTCCGCACCCGCGG
chr11R sequence	CAATTTCAACTTTAGGATTACTAGTGAAAAGATGTGCTA TTTTATAATAATAGTCAGCATCAGAAGATTTACATTCTGT TAACACATTACCAGACAATGACATTACAAAAAAGAAAC TACAGGCCAACAACTCTCACAGATACAGATGCAAAATT TTTCAAAAAATATTAACAAATCAAATTTGACTGACAATG TATAAAAAGGACTATACATTACAACCAAGTGGGATTAAT CTCAGGTATGCAAAGCTGGTTCAACATTTGTAAATCAA TTAGTATAATCTATCATATCCACAAGCTAATGAAGAAAA ATCACATGATCATATAAGTAGATACAAAAAAAGAATTTG ACTCCTGTTTATCAACACCTGTTTATCAAAAAAACTTTT GGTAACTGGGAAGAGAGGGAAACTTCCTCAACTTGAT TAAAAAAAAATCTACAAAAAAGACATGCACCTAACATTT TACTTAACAATGAGAAACTCTAAACTTTCCAGTAAGAT CAGGAATCAGGATGTTTCCTCTCACCACTGTTTCTCAA CATCATATTAGAAGTCTTAGCTAGTGCAATAATACAAGA AAAGGAAATAAAATGTATGCA

Table 2

Results of sequencing spanning 5' upstream or 3' downstream and the transgene using the primers listed in Table 1.

The forward primer was used as a sequence primer for Chr11F. Nucleotide number 6-363 was mapped on chr11: 13474269-13474589 of mm9 with 96.3% identity. The reverse primer was used as a sequence primer for Chr11R. Nucleotide number 1-82 was mapped on chr11:13474610-13474692 of mm9 with 100% identity, and 88-600 on chr1: 117315647-117316159 of hg19 with 99.9% identity.

Acknowledgments

On the completion of my work for doctoral degree, I would like to express my sincere appreciation to all people involved in. Most of all, I would like to extend a special thank to Prof. Hiromitsu Nakauchi for his mentorship to me throughout the course work. I also would like to gratefully acknowledge my collaborator, Dr. Yukio Ishii (Department of Respiratory Medicine, University of Tsukuba) for directing this project and giving me an opportunity to work with. I would like to extend my acknowledgement to Dr. Shin Kaneko for his kind mentorship to me and for a critical review of the manuscript. Additionally, I would like to thank Dr. Norihiro Kikuchi (Department of Respiratory Medicine, University of Tsukuba) for giving me critical advises on respiratory diseases as well as technical mentorship. I would like to appreciate Dr. Masataka Kasai for spending a considerable amount of his time to critically review the manuscript and Dr. Hiroshi Watarai for critically reviewing the data.

I would also like to express my special thanks to Dr. Satoshi Yamazaki for giving me critical advice. This work wouldn't go easy without help from Dr. Emiko Noguchi, who performed most of data analysis for the transgene integration site determination and Dr. Yuko Morishima, who conducted lung histological examinations (University of Tsukuba). I would like to acknowledge Dr. Tsuyoshi Ito for his assistance in microarray analysis. At the same time, I would like to thank all members of the Nakauchi Lab. for teaching me experimental techniques and for spending their time for me to discuss the results.

I would like to emphasize my gratefulness to my family member for their supports in numbers of ways. Another special thank goes to my friends. I could not complete this doctoral thesis without a support from my wife.

In ending this acknowledgement, I would like to dedicate this work to my mother in heaven as always and to my wife.